



HAL
open science

Identification of Novel Functions for Hepatitis C Virus Envelope Glycoprotein E1 in Virus Entry and Assembly

Juliano Haddad, Yves Rouillé, Xavier Hanouille, Véronique Descamps, Monzer Hamzé, Fouad Dabboussi, Thomas F. Baumert, Gilles Duverlie, Muriel Lavie, Jean Dubuisson

► **To cite this version:**

Juliano Haddad, Yves Rouillé, Xavier Hanouille, Véronique Descamps, Monzer Hamzé, et al.. Identification of Novel Functions for Hepatitis C Virus Envelope Glycoprotein E1 in Virus Entry and Assembly. *Journal of Virology*, 2017, 91 (8), pp.e00048-17. 10.1128/JVI.00048-17. hal-02112489

HAL Id: hal-02112489

<https://hal.science/hal-02112489>

Submitted on 26 Apr 2019

HAL is a multi-disciplinary open access archive for the deposit and dissemination of scientific research documents, whether they are published or not. The documents may come from teaching and research institutions in France or abroad, or from public or private research centers.

L'archive ouverte pluridisciplinaire **HAL**, est destinée au dépôt et à la diffusion de documents scientifiques de niveau recherche, publiés ou non, émanant des établissements d'enseignement et de recherche français ou étrangers, des laboratoires publics ou privés.

1 **Identification of novel functions for hepatitis C virus envelope**
2 **glycoprotein E1 in virus entry and assembly**

3 Juliano Haddad^{1,2}, Yves Rouillé¹, Xavier Hanouille³, Véronique Descamps⁴, Monzer Hamze²,
4 Fouad Dabboussi², Thomas F. Baumert⁵, Gilles Duverlie⁴, Muriel Lavie^{1*}, Jean Dubuisson^{1*}

5 1- Univ. Lille, CNRS, Inserm, CHU Lille, Institut Pasteur de Lille, U1019 - UMR 8204 -
6 CIIL- Centre d'Infection et d'Immunité de Lille, F-59000 Lille, France.

7 2- Laboratoire Microbiologie Santé et Environnement (LMSE), Ecole Doctorale en Sciences
8 et Technologie, Faculté de Santé Publique, Université Libanaise, Tripoli, Liban;

9 3- University of Lille, CNRS, UMR 8576, UGSF, Unité de Glycobiologie Structurale et
10 Fonctionnelle, F-59000 Lille, France

11 4- Laboratoire de Virologie EA4294, Centre Hospitalier Universitaire d'Amiens, Université
12 de Picardie Jules Verne, Amiens, France;

13 5- Inserm, U1110, University of Strasbourg, Pôle Hépato-digestif-Hôpitaux Universitaires de
14 Strasbourg, Strasbourg, France;

15

16 **Keywords:** hepatitis C virus; glycoprotein; envelope proteins; viral entry; viral assembly

17

18 **Running title:** HCV glycoprotein E1 functions

19 ***Corresponding authors**

20 E-mail: jean.dubuisson@ibl.cnrs.fr

21 E-mail: muriel.lavie@ibl.cnrs.fr

22 Address : Institut Pasteur de Lille, 1 rue du Prof Calmette, 59021 Lille Cedex, France

23

24 **Author contributions**

25 Conceived and designed the experiments: JH, YR, MH, FD, GD, ML, JD

26 Performed the experiments: JH, YR, VD, ML

27 Provided reagents and edited the manuscript: TFB

28 Analyzed the data: JH, YR, XH, ML, JD

29 Wrote the paper: JH, ML, JD

30 **Abstract**

31 Hepatitis C Virus (HCV) envelope glycoprotein complex is composed of E1 and E2 subunits.
32 E2 is the receptor-binding protein as well as the major target of neutralizing antibodies,
33 whereas the functions of E1 remain poorly defined. Here, we took advantage of the recently
34 published structure of the N-terminal region of E1 ectodomain to interrogate the functions of
35 this glycoprotein by mutating residues within this 79 amino acid region in the context of an
36 infectious clone. The phenotypes of the mutants were characterized to determine the effects
37 of the mutations on virus entry, replication and assembly. Furthermore, biochemical
38 approaches were also used to characterize the folding and assembly of E1E2 heterodimers.
39 Thirteen out of nineteen mutations led to viral attenuation or inactivation. Interestingly, two
40 attenuated mutants, T213A and I262A, were less dependent on claudin-1 for cellular entry in
41 Huh-7 cells. Instead, these viruses relied on claudin-6, indicating a shift in receptor
42 dependence for these two mutants in the target cell line. An unexpected phenotype was also
43 observed for mutant D263A which was no longer infectious but still showed a good level of
44 core protein secretion. Furthermore, genomic RNA was absent from these non-infectious
45 viral particles, indicating that D263A mutation leads to the assembly and release of viral
46 particles devoid of genomic RNA. Finally, a change in subcellular co-localization between
47 HCV RNA and E1 was observed for D263A mutant. This unique observation highlights for
48 the first time a crosstalk between HCV glycoprotein E1 and the genomic RNA during HCV
49 morphogenesis.

50

51

52 **Importance**

53 Hepatitis C virus (HCV) infection is a major public health problem worldwide. It encodes
54 two envelope proteins, E1 and E2, which play a major role in the life cycle of this virus. E2
55 has been extensively characterized, whereas E1 remains poorly understood. Here, we
56 investigated E1 functions by using site-directed mutagenesis in the context of the viral life
57 cycle. Our results identify unique phenotypes. Unexpectedly, two mutants clearly showed a
58 shift in receptor dependence for cell entry, highlighting a role for E1 in modulating HCV
59 particle interaction with cellular receptor(s). More importantly, another mutant led to the
60 assembly and release of viral particles devoid of genomic RNA. This unique phenotype was
61 further characterized and we observed a change in subcellular co-localization between HCV
62 RNA and E1. This unique observation highlights for the first time a crosstalk between a viral
63 envelope protein and the genomic RNA during morphogenesis.

64

65

66 **Introduction**

67 Hepatitis C virus (HCV) infection is a major public health problem with around 170 million
68 people infected worldwide (1). HCV infection has a high propensity for establishing a
69 chronic infection and, in the long term, this can lead to cirrhosis and hepatocellular
70 carcinoma. Although recent improvements in the standard of care therapy have been
71 achieved, the available treatments remain very expensive and far from being accessible to the
72 majority of HCV-infected patients (2).

73 HCV is a plus-stranded RNA virus which belongs to Hepacivirus genus in the *Flaviviridae*
74 family. The viral genome contains a single open reading frame generating a polyprotein
75 which is sequentially processed by both cellular and viral encoded proteases into ten mature
76 viral proteins. Among these polypeptides, the structural proteins (core, E1 and E2) are the
77 components of the viral particle (reviewed in (3)).

78 The E1 and E2 envelope glycoproteins are two highly glycosylated type I transmembrane
79 proteins, each with an N-terminal ectodomain and a well-conserved C-terminal
80 transmembrane domain. By being part of the viral particle, HCV envelope glycoproteins E1
81 and E2 play an essential role in virion morphogenesis as well as in HCV entry into liver cells.
82 These two steps necessitate timely and coordinated control of HCV glycoprotein functions.
83 Furthermore, HCV entry is a complex multistep process involving at least four major entry
84 factors. They include scavenger receptor BI (SR-BI)(4), tetraspanin CD81 (5) and tight-
85 junction proteins claudin-1 (CLDN1) (6), and occludin (OCLN) (7).

86 Until recently, research on HCV glycoproteins has been mainly focused on E2 because it is
87 the receptor-binding protein interacting with CD81 and SR-BI. E2 is also the major target of
88 neutralizing antibodies and it was postulated to be the fusion protein (reviewed in (8)).

89 However, the structure of E2 does not fit with what one would expect for a fusion protein (9,
90 10), suggesting that E1 alone or in association with E2 might be responsible for the fusion

91 step. Interestingly, several studies characterizing novel inhibitors of late steps of HCV entry
92 have shown that some resistant mutations can be found in E1 (11-13), re-enforcing the
93 hypothesis that this protein plays a major role during the fusion process. Furthermore, E1 also
94 plays a role in modulating the exposure of the CD81-binding region on E2 (14). Together,
95 these observations indicate that E1 plays a more important role than previously thought in the
96 HCV life cycle. It is therefore essential to better understand how E1 plays an active role in
97 HCV entry and assembly.

98 Recently, the crystal structure of the N-terminal half of E1 ectodomain has been reported
99 (15). This partial structure reveals a complex network of covalently linked, intertwined
100 homodimers. We took advantage of this reported information to investigate the functional
101 role of E1 by alanine replacement of residues in the context of an infectious clone. Among 19
102 mutants, eight showed reduced viral infectivity and five were no longer infectious.

103 Interestingly, two attenuated mutants, T213A and I262A, showed a shift of dependence for
104 virus entry factor from CLDN1 to CLDN6. Importantly, another mutation, D263A, which
105 abolished virus infectivity, led to the secretion of viral particles devoid of genomic RNA but
106 containing core protein and HCV glycoproteins, highlighting cross-talks between HCV
107 glycoprotein E1 and the genomic RNA during HCV morphogenesis.

108

109 **Results**

110 **Amino acid conservation in the N-terminal region of E1 ectodomain and mutagenesis**

111 **rationale.** The secondary structures present in the N-terminal 79 amino acid residues of E1
112 are presented in Figure 1A (15). The analysis of the E1 amino acid sequence conservation
113 among all HCV genotypes shows that the most conserved residues do not necessarily match
114 with the secondary structure elements that have been identified in the crystallographic
115 structure of the N-terminal domain of E1 ectodomain (Figure 1B). This highlights that both

116 the secondary structures and peculiar features of the loops, which contain crucial cysteine
117 residues as well as glycosylation sites, are crucial for the biological function(s) of E1. It is
118 worth noting that the less conserved region in the N-terminal region of E1 ectodomain
119 corresponds to the disordered loop between β 4 to β 5 that was not seen in the electron density
120 of the crystallographic structure.

121 Here, we mutated residues in the context of an infectious clone. The effects of mutation of
122 cysteine residues and glycosylation sites have already been reported previously (14, 16), and
123 these residues were therefore not included in this study. We produced a series of nineteen
124 mutants in which residues were individually replaced by alanine residues, and we
125 concentrated our study on structured segments (β 1 to β 5 and α -helix) or conserved amino
126 acids located close to these secondary structures (Figure 1A). Mutations were introduced in a
127 modified version of the plasmid encoding the full-length JFH1 genome in which the N-
128 terminal E1 sequence has been modified to reconstitute the A4 epitope, which is present in E1
129 of genotype 1a (17), and therefore allows the identification of E1 of genotype 2a for which
130 there is no antibody easily available. We did not introduce any mutation in β 2 since it
131 contains A4 epitope sequence. It worth noting that the introduction of the A4 epitope had no
132 effect on HCV infectivity (data not shown), indicating that this modification is not interfering
133 with the phenotype of E1 mutants characterized in our study.

134

135 **Effect of E1 mutations on HCV infectivity.** We first determined whether our mutants are
136 functional for replication. For this, we analyzed the expression of several HCV proteins at
137 48h post-electroporation. For all the mutants, the levels of expression of E2 and NS5A were
138 similar to the wild-type virus (Figure 2A). However, we observed a weaker signal for the E1
139 glycoprotein in the case of Q193A and V194A mutants, which is likely due to a weaker
140 recognition of E1 by Mab A4 whose minimum epitope has been mapped immediately

141 downstream of these two residues. Together, our data indicate that our mutations do not
142 affect HCV genome replication.

143 We then measured the effects of the mutations on the production of infectious virus by
144 determining intra- and extra-cellular infectivities. As shown in Figure 2B, we observed three
145 phenotypes for virus infectivity: (1) complete loss of infectivity, (2) no effect on infectivity or
146 (3) reduced infectivity. In β 1 strand we observed a slight decrease in extracellular infectivity
147 for Q193A and V194A, indicating that these mutations only slightly affect HCV infectivity.
148 Four mutations (S208A, T213A, V220A and L221A) in the α -helix had only a slight effect or
149 no effect at all on HCV infectivity, whereas the others had a drastic reduction in HCV
150 infectivity (I212A and Q215A) or totally abolished it (W214A and H222A). Most mutants
151 within the β -sheet (β 3 to β 5) showed no change in infectivity (G233A, M264A and V265A)
152 or only a slight decrease (R231A, V240A, P244A and I262A). However, for two of them
153 (W239A and D263A) infectivity was totally abolished. Overall, the intracellular infectivity
154 profiles were similar to those observed for extracellular viruses, excluding any effect of the
155 mutations on infectious particles release. This first analysis indicates that the α -helix and the
156 β -sheet contain essential residues for HCV infectivity.

157

158 **Determination of virion release.** To determine the effect of mutations on viral secretion in
159 the case of reduced or abolished infectivity, we measured the expression of core protein in
160 cell lysates and supernatants. As shown in Figure 3A, the levels of intracellular core protein
161 of the mutants were comparable to the wild-type, excluding any effect of the mutations on
162 HCV genomic replication. In contrast, the levels of extracellular core protein were reduced
163 for several mutants (Figure 3B). For most mutants, the levels of extracellular core protein
164 paralleled those of extracellular infectivity (compare Figures 2 and 3). However, mutant
165 D263A showed a good level of core release despite the absence of infectivity in the

166 supernatant (Figure 3B), which was confirmed in an additional experiment in the presence of
167 a mutant virus defective in virus assembly (Figure 3C), suggesting that this mutation leads to
168 the release of non-infectious viral particles.

169

170 **Effect of E1 mutations on HCV glycoproteins folding and E1E2 heterodimerization.**

171 Given the cooperativity between E1 and E2 on their respective folding, we analyzed the
172 effect of E1 mutations on the formation of E1E2 heterodimers. To study the effect of
173 mutations on the folding of E1 and E2, we used a pulldown assay using CD81-LEL that
174 recognizes correctly folded E2. As shown in Figure 4A, E2 from all the mutants was
175 recognized by CD81-LEL. However, a lower signal was observed for several of them: I212A,
176 T213A, W214A, Q215A, V220A, H222A, R231, W239A and D263A. Importantly, for some
177 mutants, the presence of E1 was not detected or barely detected (Q193A, V194A, I212A ,
178 H222A, W239A, I262A and D263A) or reduced (T213A). As discussed above, the weaker
179 E1 signal for mutants Q193A and V194A is likely due to the involvement of these two
180 residues in A4 epitope. For the other mutants, the absence or drastic decrease of E1 co-
181 precipitation suggests that these mutations affect the interaction between E1 and E2, at least
182 in the context of properly folded E2. Since these mutants (I212A, H222A, W239A, I262A
183 and D263A) are also affected in their infectivity (Figure 2B), our data suggest that the
184 assembly defect of the E1E2 heterodimer could be responsible for the decrease in infectivity.
185 However, in the case of I262A mutant, infectivity was only 1 Log₁₀ lower than the wild-type
186 (Figure 2B), suggesting that the residual interaction between E1 and E2 is sufficient to
187 maintain a certain level of infectivity. In contrast, E1 and E2 from mutants W214A and
188 Q215A were precipitated by CD81 despite loss of infectivity, suggesting that the functional
189 defect for these mutants is not due to a global effect on E1E2 folding, but rather on the virion
190 assembly itself.

191 To further characterize the folding of E1E2 complex, we also performed an
192 immunoprecipitation experiment with conformation-sensitive Mabs. We first used Mab
193 AR5A that recognizes a conformational epitope shared between E1 and E2 (18). For five of
194 our mutants (I212A, H222A, W239A, I262A and D263A), HCV glycoproteins were not
195 detected or weakly recognized by Mab AR5A (Figure 4B), which correlated with the data
196 obtained with CD81 pulldown of E1E2. Since these mutants were also altered in their
197 infectivity, one can expect that alteration in protein folding is responsible for the phenotype
198 of these viruses.

199 Finally, we also used the conformation sensitive anti-E1 Mab IGH526 whose core epitope is
200 located at amino acid positions 314-324 (19). For this analysis, we focused mainly on
201 mutants showing alterations in infectivity. As shown in Figure 4C, a decrease in the
202 recognition of E1 was observed for I212A, T213A, H222A, W239A and D263A mutants,
203 which correlated with an alteration in recognition of E1E2 complex by CD81 and AR5A
204 (Figures 4A and B). It is noteworthy, that I262A mutant was relatively well recognized by
205 IGH526 Mab (Figure 4C), which contrasts with the altered recognition by CD81 and AR5A,
206 suggesting that E1 might have achieved an advanced state of folding for this mutant despite
207 alterations in E1E2 interactions. A decrease in E1 recognition by Mab IGH526, which
208 correlated with a slight reduction of recognition by CD81, was also observed for R231A
209 mutant (Figure 4C). This could again explain the slight decrease in infectivity observed for
210 this mutant (Figures 4A).

211

212 **Effect of E1 mutations on sensitivity to antibody neutralization and inhibition by CD81**
213 **co-receptor.** The above analyzes of the effects of E1 mutations on the folding of the
214 envelope proteins were performed in the context of intracellular proteins. However,
215 incorporation of the envelope glycoproteins on the surface of the viral particle during the

216 assembly process leads to conformational changes that occur in the quaternary structure of
217 these proteins (15, 20). The biochemical analysis of the glycoproteins associated with the
218 viral particle are not easily performed because they require high amounts of viral particles. A
219 more sensitive alternative approach is to determine the sensitivity of the mutant viruses to
220 inhibition mediated by the presence of CD81-LEL or neutralizing Mabs. We therefore used
221 CD81-LEL as well as Mabs AR5A and IGH526 for these experiments. In these analyses, we
222 focused on infectious mutants showing a decrease in infectivity of approximately 1 log₁₀
223 (T213A, R231A, I262A) and S208A mutant was used as control. Interestingly, we observed a
224 strong decrease in sensitivity to inhibition by CD81-LEL, AR5A and IGH526 for T213A and
225 I262A mutants (Figure 5). These results indicate conformational changes in the envelope
226 proteins present on the surface of these two mutants, which are in line with the alterations
227 observed in our biochemical approach (Figure 4), suggesting a similar effect of the mutations
228 on the conformation of HCV glycoproteins present on the surface of the viral particle.
229 However, for some mutants, discrepancies were observed between biochemical analyses and
230 neutralization results. Indeed, R231A mutant showed some alteration in the biochemical
231 approach, but was neutralized at the wild-type level. On the opposite, I262A mutant was well
232 recognized by IGH526 in the immunoprecipitation experiment, but was much less sensitive
233 to neutralization by this antibody. This indicates that the biochemical results do not
234 necessarily parallel the functional phenotype.

235

236 **Effect of E1 mutations on the recognition of HCV receptors.** To further characterize the
237 phenotype of T213A, R231A and I262A mutants, we analyzed their dependence on known
238 receptors. For this, we analyzed the sensitivity of our mutants to inhibition by anti-receptor
239 Mabs previously reported to affect HCV entry. Similar dose-dependent decreases in
240 infectivity were observed for mutant (S208A, T213A, R231A and I262A) and wild-type

241 viruses in the presence of anti-CD81 Mab JS81 or anti-SR-BI Mab C167 (Figure 6A and B).
242 In contrast, T213A and I262A mutants were less inhibited by anti-CLDN1 Mab OM8A9-A3
243 (Figure 6C), suggesting that these viruses were less dependent on CLDN1 to infect Huh-7
244 cells. Since these cells also express CLDN6, another tight-junction protein that can be used
245 by some viruses in the absence of CLDN1 (21), we also tested the sensitivity of T213A and
246 I262A mutants to inhibition by anti-CLDN6 Mab 342927. As shown in Figure 6D, T213A
247 and I262A mutants were more sensitive than the wild-type virus to inhibition by anti-CLDN6
248 Mab, whereas S208A and R231A mutants showed the same profile as the wild-type virus
249 (data not shown). Furthermore, when we co-incubated these mutants with both anti-CLDN1
250 and anti-CLDN6 Mabs, T213A and I262A mutants were inhibited to a similar extent as the
251 wild-type virus (Figure 6E). In the absence of antibodies against OCLN, we used a cell line
252 knocked out for this receptor (22) to determine the dependence of our mutants to OCLN for
253 virus entry. None of our mutants were able to infect this cell line (data not shown), indicating
254 a similar dependence on OCLN. Altogether, our data indicate that T213A and I262A
255 mutations induce a shift in receptor usage from CLDN1 toward CLDN6.

256

257 **Characterization of the D263A mutant.** Since it had lost infectivity but showed a good
258 level of core protein secretion, D263A mutant was further characterized. For this, we
259 analyzed the released viral material on an iodixanol density gradient. As a negative control,
260 we used a viral genome carrying a large in-frame deletion in E1E2 coding region known to
261 affect the release of viral particles (Δ E1E2). The different fractions obtained after gradient
262 sedimentation were analyzed to determine infectivity as well as the content in core protein
263 and genomic RNA. As shown in Figure 7B, core protein of the wild-type virus showed two
264 peaks, one in fractions 1-2 and the other one in fractions 5-7. Fractions 1-2 corresponded to
265 the peak of infectivity and the first peak of genomic RNA, whereas fractions 5-7

266 corresponded to the second peak of genomic RNA which was non-infectious (Figure 7A).
267 Although core protein of D263A mutant was detected in fractions 1-9, the majority peaked in
268 fractions 5-7 together with the non-infectious peak of the wild type-virus (Figure 7A).
269 Surprisingly, HCV RNA was at background level for D263A mutant very similarly to the
270 control Δ E1E2 which is defective in virus assembly (Figure 7B). This was not due to the
271 absence of viral replication since intracellular RNA levels were similar for both D263A
272 mutant and wild-type virus (Figure 7C). Together, our data indicate that D263A mutation
273 leads to the assembly and release of particulate material devoid of genomic RNA.
274 To further understand the molecular basis of the absence of genomic RNA in secreted virus
275 particles in the context of D263A mutation, we investigated whether the core protein was
276 able to oligomerize into capsid-like structures. Oligomerization of core proteins expressed by
277 this mutant was analyzed on a iodixanol gradient by ultracentrifugation, as described in
278 Materials and Methods. The core protein complexes of the wild-type were detected in
279 fractions 6 to 8 (Figure 8). These fractions correspond to highly ordered multimeric
280 complexes (23). A similar profile of sedimentation was observed with D263A mutant as well
281 as with the assembly-defective control Δ E1E2 (Figure 8). However, there was a slight shift
282 towards lower density for D263A mutant. Furthermore, a small proportion of the core protein
283 was found in fractions 2 and 3 for both mutants D263A and Δ E1E2. This likely corresponds
284 to monomeric and/or dimeric forms of the core protein as previously suggested (24). When
285 the wild-type core protein was treated with 1% SDS before ultracentrifugation, only the
286 monomeric form of the core protein was detected in fractions 1 and 2 at the top of the
287 gradient. This profile is due to disruption of core protein complexes by SDS, as shown
288 previously (23) (Figure 8). These results therefore suggest that the D263A mutation does not
289 drastically affect core protein multimerization.

290 Finally, we recently showed that E1 forms homotrimers during the assembly process (20).
291 We therefore also tested the capacity of D263A mutant to form such trimers, but we did not
292 detect any defect in E1 trimerization (data not shown).

293

294 **Subcellular localization of HCV proteins during the assembly process of D263A mutant.**

295 Since D263 mutant leads to the production of viral particles devoid of genomic RNA, we
296 further investigated the subcellular co-localization of HCV proteins to determine whether this
297 mutation would induce a mislocalization of E1 glycoprotein. For this, Huh-7 cells were
298 electroporated with D263A mutant RNA, and the cells were fixed with paraformaldehyde at
299 48h post-electroporation before being processed for immunofluorescence. E1 mutated at
300 position D263 showed a co-localization with E2 similar to what was observed for the wild-
301 type virus (Figure 9). Furthermore, there was no difference in core and NS5A co-localization
302 with lipid droplets, the site where HCV assembly is supposed to take place (25). Finally, we
303 also analyzed whether D263A mutation affects the colocalization of core or E1 with the viral
304 RNA. For this, we analyzed the localization of HCV RNA by FISH. Although D263A
305 mutation did not change the co-localization of core protein with HCV RNA (Figure 10A), a
306 significant decrease in subcellular co-localization between HCV RNA and E1 was observed
307 for this mutant (Figure 10B and C), supporting the hypothesis that E1 could play a role in the
308 recruitment of HCV RNA during virus assembly

309

310 **Discussion**

311 For a long time, E1 remained poorly studied. However, recent structural studies on E2
312 suggest that E1 might play an active role in the fusion process (26), prompting us to initiate a
313 functional study of this protein based on the recently published structure of its N-terminus
314 (15). Our data identify residues in the α -helix and the β -sheet that are important for the

315 assembly and release of infectious viral particles. Characterization of our mutants also
316 highlights crosstalks between E1 and E2 during HCV morphogenesis. Furthermore,
317 neutralization experiments indicate that mutations in two of our mutants induce a shift in
318 receptor usage from CLDN1 toward CLDN6. Finally, characterization of the mutant D263A
319 shows that this virus leads to assembly and release of viral particles devoid of genomic RNA,
320 indicating that E1 plays a role in the incorporation of HCV RNA into the nucleocapsid.

321 Several mutations in E1 affect the folding of E2. This is the case for I212A , T213A, H222A
322 and W239A mutants, as shown by CD81 pulldown. CD81 is often used as a probe to
323 determine the folding of E2 since its binding region is located in E2 and it is conformation
324 dependent (27). HCV glycoproteins have been shown to assemble as a noncovalent E1E2
325 heterodimer (28), and these proteins are known to cooperate for the formation of a functional
326 complex(29). The folding of E1 has indeed initially been shown to be dependent on the co-
327 expression of E2 (30, 31). Later on, it was reported that E1 can also affect the folding of E2
328 (32, 33). Our observation that mutations in E1 can affect the recognition of E2 by CD81 is
329 therefore in line with the fact that E1 can play an active role in the folding of E2 in the
330 context of E1E2. It is however to be noted that E2 expressed alone is well recognized by
331 CD81(5), suggesting that mutations in E1 can push E2 towards a conformation poorly
332 recognized by CD81, which is in line with the crosstalks observed between these two proteins
333 (34, 35). I212, T213 and H222 correspond to highly conserved residues located in the α -helix
334 of E1 (Figure 11), whereas W239 belongs to the β 4 strand.

335 Several mutations in E1 affect E1E2 interaction. This is particularly the case for mutants
336 W239A, I262A and D263A, as shown by the lack of E1 signal after CD81 pulldown.
337 Residues involved in E1E2 interactions have been identified in the transmembrane domains
338 of these two proteins (36). Moreover, a study based on chimeric E1E2 heterodimers derived

339 from different genotypes has also recently identified residues in the ectodomain of E1, at
340 positions 308, 330 and 345, as being involved in functional interactions between E1 and E2
341 (35). However, in the study of Douam and coworkers, no biochemical analysis was
342 performed to determine the physical interaction between these two proteins. Amino acid
343 residues W239A, I262A and D263A identified in our study as affecting E1E2 interaction are
344 located in a β -sheet structure identified in the N-terminal region of E1 (Figure 11) (15). I262,
345 D263 and W239 belong to the β 4 and β 5 strands respectively and are close in space in the
346 structure of E1. Indeed the D263 residue is directly facing the W239 residue. Therefore, our
347 data suggest that this β -sheet is involved in interactions with E2. Interestingly, D263 and
348 W239, two highly conserved residues, are part of a rather hydrophobic surface that has been
349 described by El Omari *et al.* as being likely involved in interaction with another protein
350 partner (15). It has to be noted that one of our mutations, I262A, is not lethal for the virus,
351 suggesting that alteration in E1E2 interactions does not necessarily abolish viral infectivity.
352 However, for this particular mutant, E1E2 interaction was not totally abolished, and the
353 remaining infectivity might be explained by this residual interaction. If I262 is close to D263
354 and W239 residues, its side-chain does not point out in the same direction. Indeed, the side-
355 chains of D263 and W239 are exposed to the E1 surface, directly available to potentially
356 interact with another protein, whereas the side-chain of I262 is buried in the E1 structure and
357 makes hydrophobic contacts with the α -helix (Figure 11). Thus the side-chain of I262 is
358 unlikely to be directly involved in the interaction with E2, and this may explain the peculiar
359 phenotype observed for I262 mutant.

360 Our data indicate that mutations in E1 can affect the tropism of HCV for CLDN1. Indeed,
361 T213A and I262A mutants preferentially use CLDN6 instead of CLDN1 in Huh-7 cells. A
362 similar shift in receptor dependence has recently been reported for another E1 mutant that has
363 been selected by long-term culturing and passage of the HCV Jc1 isolate through CLDN1

364 KO Huh-7.5 cells (37). Together, these data point to a role for E1 in the HCV cell-entry
365 process as a modulator of entry factor usage. It has been previously reported that many HCV
366 isolates can naturally use both CDLN1 and CLDN6 for host cell entry (21, 38-40) , so a
367 change in receptor dependence from CLDN1 to CLDN6 is not entirely surprising. However,
368 it is not clearly known whether E1 interacts directly with CLDN1. It has been reported that
369 mutations in E1 that affect the infectivity of pseudoparticles bearing HCV glycoproteins can
370 modulate the binding of these particles to CLDN1-expressing cells, suggesting a role for E1
371 in HCV glycoprotein interaction with CLDN1 (35). However, one cannot exclude that these
372 E1 mutations may be functioning indirectly by influencing how E2 interacts with CLDN1.
373 We have indeed already observed that mutations in E1 can affect E2-CD81 interaction,
374 indicating that E1 plays a role in modulating the receptor binding capacity of E2 (14). The
375 most surprising observation is that mutations located in different regions of the E1 primary
376 sequence can affect the dependence on CLDN1. Indeed, the mutations identified in our work
377 are at position 213 and 262 which belong to the α -helix and the β 5 strand respectively
378 (Figure 1), whereas the mutation identified by the group of Evans is located at position 316
379 (37), which is located in the epitope of neutralizing Mab IGH526 (19). However, T213 in the
380 α -helix and I262 in the β 5 strand are proximate in space in the E1 structure. Moreover, I262
381 establishes hydrophobic interactions with the α -helix that contribute to the folding back of
382 this helix on the β -sheet of E1 (Figure 11). Interestingly, our biochemical and neutralization
383 data indicate that both T213A and I262A mutations affect E1 recognition by IGH526,
384 suggesting that amino acid positions 213, 262 and 316 might be in close proximity in the 3D
385 structure of E1. Whether the alteration in CLDN1-dependence is clinically relevant remains
386 to be determined.

387 The most surprising observation of our study is the production of HCV particles devoid of
388 genomic RNA in the case of D263A mutation. The D263 amino acid is highly conserved.

389 Indeed, an aspartate residue is present at this position in 18 out of 19 reference sequences
390 from all confirmed genotypes and subtypes (Figure 1B) as well as in 96% of the full E1
391 sequences from the euHCVdb (<https://euhcvdb.ibcp.fr>)(41)1. It has been shown that, in a cell-
392 free assay, HCV core proteins produced in bacteria self-assemble into nucleocapsids (42).
393 However, in this case viral or nonviral RNA molecules were associated with the particles.
394 Intracellular assembly of HCV capsids has also been described in the past (43). However,
395 these particles were not secreted and they were shown to form abortive budding events. In
396 our case, we detected secretion of viral particles that contain at least the core protein but no
397 genomic RNA. Due to the low production of particles and the fact that we cannot amplify
398 them by reinfection, we could not determine whether HCV envelope glycoproteins are
399 associated with these particles. We presume that they should be present in the envelope. E1
400 has been shown to interact with the capsid protein in the context of a heterologous expression
401 system, at least after oligomerization of the capsid protein (44). Together with our data, this
402 suggests that E1 plays a major role in HCV particle assembly. In the context of our D263A
403 mutant, one can speculate that due to loss of interaction with E2, E1 might be able to directly
404 interact with the capsid protein in the absence of interaction with the genomic RNA.
405 Interestingly, we also observed a decrease in subcellular co-localization between HCV RNA
406 and E1 for D263A mutant which is in line with the hypothesis that, through its interaction
407 with core protein, E1 might play a role in recruiting the genomic RNA. As already mentioned
408 above, in the E1 structure, the D263 residue that is located in the β -sheet has its side chain
409 exposed at the molecular surface (Figure 11). Interestingly, the D263 carboxylic function of
410 its side chain is at the center of a hydrogen bonds network, which comprises the R237, W239
411 and H261 side chains (Figure 11B). This polar interaction network might be involved in the
412 stabilization of D263, R237, W239 and H261 side chains toward an E1 conformation suitable
413 to interact with an essential biological partner.

414 To conclude, our mutagenesis study highlights cross-talks between the E1 and E2 during
415 HCV morphogenesis. Our data also indicate the role of E1 in modulating functional
416 interactions between E1E2 complex and CLDN1. Finally, this study describes for the first
417 time a cross-talk between E1 and the genomic RNA during HCV morphogenesis.

418

419 **Materials and Methods**

420 **Cell culture.** Huh-7 hepatoma cells (45) were grown in Dulbecco's modified essential
421 medium (DMEM; Thermofisher) supplemented with glutamax, 10% fetal calf serum and non
422 essential aminoacids (NEAA).

423 **Antibodies.** Anti-HCV monoclonal antibodies (Mabs) A4 (anti-E1) (46) and 3/11 (anti-E2;
424 kindly provided by J. A. McKeating, University of Birmingham, Birmingham, UK)(47) were
425 produced *in vitro* by using a MiniPerm apparatus (Heraeus) as recommended by the
426 manufacturer. Anti-E1E2 Mabs AR5A (18) and anti-E1 Mab IGH526 (19) were kindly
427 provided by M. Law (Scripps Research Institute, La Jolla, CA, USA). The anti-NS5A MAb
428 9E10 (48) and a polyclonal antibody (49) were a gift from C. M. Rice (Rockefeller
429 University, New York, NY) and M. Harris (University of Leeds, United Kingdom),
430 respectively. Anti-core Mab ACAP-27 (50) was kindly provided by J. F. Delagneau (Bio-
431 Rad, France). Anti-SR-BI Mab C167 was a gift from A. Nicosia (Okairos, Rome Italy) (51).
432 Anti-CLDN1 Mab OM8A9-A3 has been previously described (52). Commercially available
433 anti-CD81 Mab JS81 (BD Pharmingen), anti-SR-BI polyclonal antibody (Abcam) and anti-
434 CLDN6 Mab clone 342927 (R&D Systems) were used in this work. Secondary antibodies
435 used for immunofluorescence were purchased from Jackson ImmunoResearch. Control anti-
436 tubulin antibody was from Sigma.

437 **Structural model of E1.** The structural model of the N-terminal region of E1 ectodomain was
438 constructed using the JFH1 amino acid sequence and the crystallographic structure of E1
439 from H77 strain (PDB code 4UOI, chain F) as template thanks to the Swiss-Model server
440 (53).

441 **Mutagenesis and virus production.** The virus used in this study is a modified version of the
442 JFH1 isolate (genotype 2a; GenBank accession number AB237837) (54), kindly provided by
443 T. Wakita (National Institute of Infectious Diseases, Tokyo, Japan) (17). Mutants were
444 generated by site-directed mutagenesis. Selected residues were replaced by alanines. The
445 restriction enzyme XbaI was used to linearize plasmids encoding viral RNAs. The linearized
446 plasmids were then treated with mung bean nuclease (New England BioLabs) with the aim of
447 obtaining blunt-ended DNA. For *in vitro* transcription, 2 µg of linearized DNA was
448 transcribed using the Megascript kit according to the manufacturer's protocol (Ambion). The
449 *in vitro* transcription reaction mixture was set up and incubated at 37°C for 4 h, and
450 transcripts were precipitated by the addition of equal volumes of LiCl and nuclease-free
451 water. The mixture was chilled at - 20°C for 30 min and then centrifuged at 4°C for 15 min at
452 14,000 g. The supernatants were then removed, and the RNA pellets were washed with 70%
453 ethanol and resuspended in RNase-free water. Infectivity analyses were performed as
454 previously described (14). Briefly, supernatants containing extracellular virus were removed
455 at different times after electroporation, and cell debris was removed by centrifugation for 5
456 min at 10,000 x g. Infected cells were washed with phosphate-buffered saline (PBS),
457 harvested by treatment with trypsin, and intracellular viral particles were obtained after 4
458 freeze-thaw cycles. Cell lysates were clarified by centrifugation at 10,000 x g for 7 min.
459 Clarified supernatants containing extracellular virus and intracellular virus were used for
460 infection of naïve Huh-7 cells. Infected cells were then fixed with ice-cold methanol (100%)
461 and immunostained with anti-E1 or anti-NS5A antibodies. The non replicative control HCV

462 genome (GND) contained a GND mutation in the NS5B active site, as previously reported
463 (55). The assembly-deficient control of HCV (Δ E1E2) containing an in-frame deletion
464 introduced into the E1E2 regions has been previously described (54).

465 ***Immunofluorescence.*** Immunofluorescence analyses were performed as previously
466 described (24). Briefly, Huh-7 cells electroporated with 10 μ g of wild-type or mutant RNAs,
467 were grown on 12-mm coverslips or in 96 well plates. After 48 h, the cells were washed
468 twice with PBS and then fixed with cold methanol (100%) for 5 min. The methanol was
469 removed by washing the cells twice with PBS. The cells were then blocked with 10% goat or
470 horse serum for at least 10 min, followed by washing with PBS. The primary anti-E1, anti-E2
471 and anti-NS5A antibodies were diluted in 10% goat serum/horse serum, and the coverslips
472 were incubated with antibodies at room temperature for 25 min. The cells were then washed
473 3 times in PBS. The secondary antibody was diluted in goat serum/horse serum (1/500), and
474 coverslips were incubated with a Cy3-conjugated antibody for 20 min. The cells were washed
475 again with PBS. Nuclei were stained with DAPI (4',6-diamidino-2-phenylindole). The
476 coverslips were mounted on glass slides using 7 μ L of mounting medium (Mowiol 4-88,
477 Calbiochem). Confocal microscopy was performed with a LSM 880 confocal laser-scanning
478 microscope (Zeiss) using a x63/1.4 numerical aperture oil immersion lens. Double-label
479 immunofluorescence signals were sequentially collected by using single fluorescence
480 excitation and acquisition settings to avoid crossover. Images were processed by using Image
481 J software.

482 ***Equilibrium density gradient analysis.*** Equilibrium density gradient analyses were
483 performed as previously described (14) after concentration of viral preparation by
484 polyethylene glycol precipitation as described (56). Briefly, viruses were harvested 48 h
485 following electroporation. Approximately 80 mL of virus supernatants was precipitated using
486 polyethylene glycol (PEG) 6000 to a final concentration of 8%. The mixture was shaken for 1

487 h on ice, centrifuged at 8,000 rpm (Beckman JLA-10.5 rotor) for 25 min, and then
488 resuspended in 1 mL sterile PBS. The virus was then loaded on a 10-50% iodixanol gradient.
489 The gradients were spun for 16 h at 36,000 rpm in an SW41 rotor (Beckman) and
490 fractionated from the top.

491 **Core oligomerization.** Huh-7 cells electroporated with mutant and wild-type RNA genomes
492 were lysed at 48 h postelectroporation in lysis buffer (PBS/0.3% NP-40 and a protease
493 inhibitor cocktail (Roche)) for 15 min at room temperature. Cell lysates were precleared by
494 centrifugation at 14,000 rpm for 5 min at 4°C. Each sample was layered on top of 11 ml 10-
495 50 % iodixanol gradient and centrifuged in a Beckman SW41 Ti rotor (Beckman) at 36,000
496 rpm for 16 h at 4°C. Fractions of 1 ml were collected from the top of each tube and analyzed
497 by SDS-PAGE and immunoblotting.

498 **HCV core quantification.** HCV core was quantified by a fully automated chemiluminescent
499 microparticle immunoassay according to the manufacturer's instructions (Architect HCVAg;
500 Abbott, Germany) as previously described (57, 58).

501 **Western blotting.** Western blotting experiments were performed as previously described (13).
502 Cells were lysed in PBS lysis buffer (1% Triton X-100, 20 mM NEM, 2 mM EDTA, protease
503 inhibitor cocktail; Roche). Cell lysates were then precleared by centrifugation at 14,000 x g
504 for 5 min at 4°C. Protein samples were heated for 7 min at 70°C in Laemmli sample buffer.
505 Following separation with SDS-PAGE, the proteins were transferred onto nitrocellulose
506 membranes (Hybond-ECL; Amersham) and detected with specific antibodies. Following
507 incubation with primary antibodies, the membranes were incubated with the corresponding
508 peroxidase-conjugated anti-rat (Jackson), anti-rabbit (Amersham), anti-sheep (Amersham) or
509 anti-mouse (Dako) antibodies. The proteins were then detected by enhanced
510 chemiluminescence (ECL) (Amersham) as recommended by the manufacturer.

511 **CD81 interaction and immunoprecipitation assays.** CD81 pulldown and

512 immunoprecipitation experiments were performed as previously described (59). Cells were
513 lysed in PBS lysis buffer (1% Triton X-100, 20 mM NEM, 2 mM EDTA, protease inhibitor
514 cocktail; Roche). Cell lysates were then cleared by centrifugation at 14,000 x g for 15 min at
515 4°C. For CD81 pulldown, Glutathione-Sepharose beads (glutathione-Sepharose 4B;
516 Amersham Bioscience) were washed twice with cold PBS to remove the storage buffer. For
517 each cell lysate sample, 50 µL of glutathione beads was incubated with 10 µg of human
518 CD81 (hCD81) large extracellular loop (LEL) glutathione *S*-transferase (GST) recombinant
519 protein in 1 mL cold PBS containing 1% Triton X-100 for 2 h at 4°C. Following incubation,
520 the glutathione-Sepharose beads were washed with cold PBS. Cell lysate samples containing
521 E1E2 proteins were then incubated with CD81-LEL complexed with glutathione beads
522 overnight at 4°C. The following day, the beads were washed five times with cold PBS and
523 1% Triton X-100. Finally, the beads were resuspended in 30 µL of Laemmli buffer. Samples
524 were heated at 70°C and loaded onto 10% SDS-PAGE, followed by western blotting to
525 reveal the proteins of interest. For immunoprecipitation, 70 µL of protein A Sepharose beads
526 was incubated with 10 µg of Rabbit anti-human IgG (Dako) in 1 mL cold PBS and 1%
527 Triton X-100 for 2 h at 4°C. In parallel, 100 µL of cell lysates were incubated with 2 µg of
528 Mab AR5A (anti-E1E2) or Mab IGH526 (anti-E1) in 400 µL cold PBS and 1% Triton X-100
529 for 2 h at 4°C. Next, Protein A Sepharose beads were washed twice with cold PBS and 1%
530 Triton X-100 and added to cell lysates. The mixture was then incubated for 90 min at 4°C.
531 After incubation, the beads were washed five times with cold PBS and 1% Triton X-100.
532 Finally, the beads were resuspended in 30 µL of Laemmli buffer. The presence of HCV
533 envelope glycoproteins was then detected by western blotting.

534 ***Entry inhibition assays and neutralization assays.*** Viruses or cells were preincubated with
535 human CD81-LEL, Mab AR5A, Mab IGH526 or anti-receptor antibodies for 2 h at 37°C.
536 The viruses were then put in contact with Huh-7 cells. At 6 h post-infection, the inoculum

537 was removed and the cells were further incubated for 72 h with complete medium. The cells
538 were then processed for immunofluorescence to measure residual infectivity.

539 ***Fluorescence in situ hybridization (FISH) and colocalization with viral proteins.*** In Situ
540 hybridization was performed as previously described (60). Briefly, cells were washed once
541 with PBS and fixed with 500 µl of 4% paraformaldehyde for 20 min at room temperature,
542 followed by three times washing with PBS. Fixed cells were processed for FISH analysis,
543 using the QuantiGene ViewRNA ISH Cell Assay (Affymetrix) as recommended by the
544 manufacturer.

545 ***Graphs and statistics.*** Prism v5.0c (GraphPad Software Inc., La Jolla, CA) software was
546 used to prepare graphs and to determine statistical significance of differences between data
547 sets using the Mann-Whitney test.

548

549

550 **Acknowledgements**

551 We thank J. F. Delagneau, M. Harris, M. Law, J. McKeating, A. Nicosia, C. Rice and T.
552 Wakita for providing essential reagents. We also thank Sophana Ung for his help in preparing
553 the figures. The immunofluorescence analyses were performed with the help of the imaging
554 core facility of the BioImaging Center Lille Nord-de-France.

555 This work was supported by the French National Agency for Research on AIDS and Viral
556 Hepatitis (ANRS) and the ANR through ERA-NET Infect-ERA program (ANR-13-IFEC-
557 0002-01). Juliano Haddad was successively supported by a fellowship from the Lebanese
558 development association and from the ANRS.

559

560

561

562 **References**

- 563 1. **Mohd Hanafiah K, Groeger J, Flaxman AD, Wiersma ST.** 2013. Global
564 epidemiology of hepatitis C virus infection: New estimates of age-specific antibody to
565 HCV seroprevalence. *Hepatology* **57**:1333–1342.
- 566 2. **Webster DP, Klenerman P, Dusheiko GM.** 2015. Hepatitis C. *The Lancet*
567 **385**:1124–1135.
- 568 3. **Popescu CI, Riva L, Vlaicu O, Farhat R, Rouillé Y, Dubuisson J.** 2014. Hepatitis C
569 Virus Life Cycle and Lipid Metabolism. *Biology* **3**:892–921.
- 570 4. **Scarselli E, Ansuini H, Cerino R, Roccasecca RM, Acali S, Filocamo G, Traboni**
571 **C, Nicosia A, Cortese R, Vitelli A.** 2002. The human scavenger receptor class B type
572 I is a novel candidate receptor for the hepatitis C virus. *EMBO J* **21**:5017–5025.
- 573 5. **Pileri P, Uematsu Y, Campagnoli S, Galli G, Falugi F, Petracca R, Weiner AJ,**
574 **Houghton M, Rosa D, Grandi G, Abrignani S.** 1998. Binding of hepatitis C virus to
575 CD81. *Science* **282**:938–941.
- 576 6. **Evans MJ, von Hahn T, Tscherne DM, Syder AJ, Panis M, Wölk B, Hatzioannou**
577 **T, McKeating JA, Bieniasz PD, Rice CM.** 2007. Claudin-1 is a hepatitis C virus co-
578 receptor required for a late step in entry. *Nature* **446**:801–805.
- 579 7. **Ploss A, Evans MJ, Gaysinskaya VA, Panis M, You H, de Jong YP, Rice CM.**
580 2009. Human occludin is a hepatitis C virus entry factor required for infection of
581 mouse cells. *Nature* **457**:882–886.
- 582 8. **Lavie M, Penin F, Dubuisson J.** 2015. HCV envelope glycoproteins in virion
583 assembly and entry. *Future Virol* **10**:297–312.

- 584 9. **Khan AG, Whidby J, Miller MT, Scarborough H, Zatorski AV, Cygan A, Price**
585 **AA, Yost SA, Bohannon CD, Jacob J, Grakoui A, Marcotrigiano J.** 2014.
586 Structure of the core ectodomain of the hepatitis C virus envelope glycoprotein 2.
587 Nature **509**:381–384.
- 588 10. **Kong L, Giang E, Nieuwma T, Kadam RU, Cogburn KE, Hua Y, Dai X, Stanfield**
589 **RL, Burton DR, Ward AB, Wilson IA, Law M.** 2013. Hepatitis C Virus E2
590 Envelope Glycoprotein Core Structure. Science **342**:1090–1094.
- 591 11. **Perin PM, Haid S, Brown RJP, Doerrbecker J, Schulze K, Zeilinger C, von**
592 **Schaewen M, Heller B, Vercauteren K, Luxenburger E, Baktash YM, Vondran**
593 **FW, Speerstra S, Awadh A, Mukhtarov F, Schang LM, Kirschning A, Müller R,**
594 **Guzman CA, Kaderali L, Randall G, Meuleman P, Ploss A, Pietschmann T.** 2016.
595 Flunarizine prevents hepatitis C virus membrane fusion in a genotype-dependent
596 manner by targeting the potential fusion peptide within E1. Hepatology **63**:49–62.
- 597 12. **Vausselin T, Calland N, Belouzard S, Descamps V, Douam F, Helle F, François C,**
598 **Lavillette D, Duverlie G, Wahid A, Fénéant L, Cocquerel L, Guérardel Y,**
599 **Wychowski C, Biot C, Dubuisson J.** 2013. The antimalarial ferroquine is an inhibitor
600 of hepatitis C virus. Hepatology **58**:86–97.
- 601 13. **Vausselin T, Séron K, Lavie M, Mesalam AA, Lemasson M, Belouzard S, Fénéant**
602 **L, Danneels A, Rouillé Y, Cocquerel L, Foquet L, Rosenberg AR, Wychowski C,**
603 **Meuleman P, Melnyk P, Dubuisson J.** 2016. Identification of a New Benzimidazole
604 Derivative as an Antiviral against Hepatitis C Virus. J Virol **90**:8422–8434.
- 605 14. **Wahid A, Helle F, Descamps V, Duverlie G, Penin F, Dubuisson J.** 2013. Disulfide
606 Bonds in Hepatitis C Virus Glycoprotein E1 Control the Assembly and Entry

- 607 Functions of E2 Glycoprotein. *J Virol* **87**:1605–1617.
- 608 15. **El Omari K, Iourin O, Kadlec J, Sutton G, Harlos K, Grimes JM, Stuart DI.**
609 2014. Unexpected structure for the N-terminal domain of hepatitis C virus envelope
610 glycoprotein E1. *Nat Commun* **5**:1–5.
- 611 16. **Helle F, Vieyres G, Elkrief L, Popescu CI, Wychowski C, Descamps V, Castelain**
612 **S, Roingeard P, Duverlie G, Dubuisson J.** 2010. Role of N-linked glycans in the
613 functions of hepatitis C virus envelope proteins incorporated into infectious virions. *J*
614 *Virol* **84**:11905–11915.
- 615 17. **Goueslain L, Alsaleh K, Horellou P, Roingeard P, Descamps V, Duverlie G,**
616 **Ciczora Y, Wychowski C, Dubuisson J, Rouille Y.** 2010. Identification of GBF1 as
617 a Cellular Factor Required for Hepatitis C Virus RNA Replication. *J Virol* **84**:773–
618 787.
- 619 18. **Giang E, Dorner M, Prentoe JC, Dreux M, Evans MJ, Bukh J, Rice CM, Ploss A,**
620 **Burton DR, Law M.** 2012. Human broadly neutralizing antibodies to the envelope
621 glycoprotein complex of hepatitis C virus. *Proc Natl Acad Sci USA* **109**:6205–6210.
- 622 19. **Kong L, Kadam RU, Giang E, Ruwona TB, Nieuwma T, Culhane JC, Stanfield**
623 **RL, Dawson PE, Wilson IA, Law M.** 2015. Structure of Hepatitis C Virus Envelope
624 Glycoprotein E1 Antigenic Site 314–324 in Complex with Antibody IGH526. *J Mol*
625 *Biol* **427**:2617–2628.
- 626 20. **Falson P, Bartosch B, Alsaleh K, Tews BA, Loquet A, Ciczora Y, Riva L,**
627 **Montigny C, Montpellier C, Duverlie G, Pécheur E-I, le Maire M, Cosset FL,**
628 **Dubuisson J, Penin F.** 2015. Hepatitis C Virus Envelope Glycoprotein E1 Forms
629 Trimers at the Surface of the Virion. *J Virol* **89**:10333–10346.

- 630 21. **Haid S, Grethe C, Dill MT, Heim M, Kaderali L, Pietschmann T.** 2014. Isolate-
631 dependent use of claudins for cell entry by hepatitis C virus. *Hepatology* **59**:24–34.
- 632 22. **Shirasago Y, Shimizu Y, Tanida I, Suzuki T, Suzuki R, Sugiyama K, Wakita T,**
633 **Hanada K, Yagi K, Kondoh M, Fukasawa M.** 2016. Occludin-Knockout Human
634 Hepatic Huh7.5.1-8-Derived Cells Are Completely Resistant to Hepatitis C Virus
635 Infection. *Biol Pharm Bull* **39**:839–848.
- 636 23. **Ai LS, Lee YW, Chen SS.** 2009. Characterization of Hepatitis C Virus Core Protein
637 Multimerization and Membrane Envelopment: Revelation of a Cascade of Core-
638 Membrane Interactions. *J Virol* **83**:9923–9939.
- 639 24. **Alsaleh K, Delavalle PY, Pillez A, Duverlie G, Descamps V, Rouille Y, Dubuisson**
640 **J, Wychowski C.** 2010. Identification of Basic Amino Acids at the N-Terminal End of
641 the Core Protein That Are Crucial for Hepatitis C Virus Infectivity. *J Virol* **84**:12515–
642 12528.
- 643 25. **Miyanari Y, Atsuzawa K, Usuda N, Watashi K, Hishiki T, Zayaz M,**
644 **Bartenschlager R, Wakita T, Hijikata M, Shimotohno K.** 2007. The lipid droplet
645 is an important organelle for hepatitis C virus production. *Nat Cell Biol* **9**: 1089-1097.
646
- 647 26. **Li Y, Modis Y.** 2014. A novel membrane fusion protein family in Flaviviridae?
648 *Trends Microbiol* **22**:176–182.
- 649 27. **Cocquerel L, Voisset C, Dubuisson J.** 2006. Hepatitis C virus entry: potential
650 receptors and their biological functions. *J Gen Virol* **87**:1075–1084.
- 651 28. **Deleersnyder V, Pillez A, Wychowski C, Blight K, Xu J, Hahn YS, Rice CM,**
652 **Dubuisson J.** 1997. Formation of native hepatitis C virus glycoprotein complexes. *J*

- 653 Virol **71**:697–704.
- 654 29. **Lavie M, Goffard A, Dubuisson J.** 2007. Assembly of a functional HCV
655 glycoprotein heterodimer. *Curr Issues Mol Biol* **9**:71–86.
- 656 30. **Michalak JP, Wychowski C, Choukhi A, Meunier JC, Ung S, Rice CM,**
657 **Dubuisson J.** 1997. Characterization of truncated forms of hepatitis C virus
658 glycoproteins. *J Gen Virol* **78 (Pt 9)**:2299–2306.
- 659 31. **Patel J, Patel AH, McLauchlan J.** 2001. The Transmembrane Domain of the
660 Hepatitis C Virus E2 Glycoprotein Is Required for Correct Folding of the E1
661 Glycoprotein and Native Complex Formation. *Virology* **279**:58–68.
- 662 32. **Brazzoli M, Helenius A, Fong SK, Houghton M, Abrignani S, Merola M.** 2005.
663 Folding and dimerization of hepatitis C virus E1 and E2 glycoproteins in stably
664 transfected CHO cells. *Virology* **332**:438–453.
- 665 33. **Cocquerel L, Quinn ER, Flint M, Hadlock KG, Fong SK, Levy S.** 2003.
666 Recognition of native hepatitis C virus E1E2 heterodimers by a human monoclonal
667 antibody. *J Virol* **77**:1604–1609.
- 668 34. **Albecka A, Montserret R, Krey T, Tarr AW, Diesis E, Ball JK, Descamps V,**
669 **Duverlie G, Rey F, Penin F, Dubuisson J.** 2011. Identification of New Functional
670 Regions in Hepatitis C Virus Envelope Glycoprotein E2. *J Virol* **85**:1777–1792.
- 671 35. **Douam F, Dao Thi VL, Maurin G, Fresquet J, Mompelat D, Zeisel MB, Baumert**
672 **TF, Cosset FL, Lavillette D.** 2014. Critical interaction between E1 and E2
673 glycoproteins determines binding and fusion properties of hepatitis C virus during cell
674 entry. *Hepatology* **59**:776–788.

- 675 36. **Op De Beeck A, Montserret R, Duvet S, Cocquerel L, Cacan R, Barberot B, Le**
676 **Maire M, Penin F, Dubuisson J.** 2000. The Transmembrane Domains of Hepatitis C
677 Virus Envelope Glycoproteins E1 and E2 Play a Major Role in Heterodimerization. *J*
678 *Biol Chem* **275**:31428–31437.
- 679 37. **Hopcraft SE, Evans MJ.** 2015. Selection of a hepatitis C virus with altered entry
680 factor requirements reveals a genetic interaction between the E1 glycoprotein and
681 claudins. *Hepatology* **62**:1059–1069.
- 682 38. **Zheng A, Yuan F, Li Y, Zhu F, Hou P, Li J, Song X, Ding M, Deng H.** 2007.
683 Claudin-6 and Claudin-9 Function as Additional Coreceptors for Hepatitis C Virus. *J*
684 *Virol* **81**:12465–12471.
- 685 39. **Meertens L, Bertaux C, Cukierman L, Cormier E, Lavillette D, Cosset FL,**
686 **Dragic T.** 2008. The Tight Junction Proteins Claudin-1, -6, and -9 Are Entry Cofactors
687 for Hepatitis C Virus. *J Virol* **82**:3555–3560.
- 688 40. **Fofana I, Zona L, Thumann C, Heydmann L, Durand SC, Lupberger J, Blum**
689 **HE, Pessaux P, Gondeau C, Reynolds GM, McKeating JA, Grunert F, Thompson**
690 **J, Zeisel MB, Baumert TF.** 2013. Functional Analysis of Claudin-6 and Claudin-9 as
691 Entry Factors for Hepatitis C Virus Infection of Human Hepatocytes by Using
692 Monoclonal Antibodies. *J Virol* **87**:10405–10410.
- 693 41. **Combet C, Garnier N, Charavay C, Grando D, Crisan D, Lopez J, Dehne-Garcia**
694 **A, Geourjon C, Bettler E, Hulo C, Le Mercier P, Bartenschlager R, Diepolder H,**
695 **Moradpour D, Pawlotsky JM, Rice CM, Trépo C, Penin F, Deléage G.** 2007.
696 euHCVdb: the European hepatitis C virus database. *Nucleic Acids Res* **35**:D363–6.
- 697 42. **Kunkel M, Lorinczi M, Rijnbrand R, Lemon SM, Watowich SJ.** 2001. Self-

- 698 assembly of nucleocapsid-like particles from recombinant hepatitis C virus core
699 protein. *J Virol* **75**:2119–2129.
- 700 43. **Blanchard E, Brand D, Trassard S, Goudeau A, Roingeard P.** 2002. Hepatitis C
701 virus-like particle morphogenesis. *J Virol* **76**:4073–4079.
- 702 44. **Nakai K, Okamoto T, Kimura-Someya T, Ishii K, Lim CK, Tani H, Matsuo E,**
703 **Abe T, Mori Y, Suzuki T, Miyamura T, Nunberg JH, Moriishi K, Matsuura Y.**
704 2006. Oligomerization of Hepatitis C Virus Core Protein Is Crucial for Interaction with
705 the Cytoplasmic Domain of E1 Envelope Protein. *J Virol* **80**:11265–11273.
- 706 45. **Nakabayashi H, Taketa K, Miyano K, Yamane T, Sato J.** 1982. Growth of human
707 hepatoma cells lines with differentiated functions in chemically defined medium.
708 *Cancer Res* **42**:3858–3863.
- 709 46. **Dubuisson J, Hsu HH, Cheung RC, Greenberg HB, Russell DG, Rice CM.** 1994.
710 Formation and intracellular localization of hepatitis C virus envelope glycoprotein
711 complexes expressed by recombinant vaccinia and Sindbis viruses. *J Virol* **68**:6147–
712 6160.
- 713 47. **Flint M, Maidens C, Loomis-Price LD, Shotton C, Dubuisson J, Monk P,**
714 **Higginbottom A, Levy S, McKeating JA.** 1999. Characterization of hepatitis C virus
715 E2 glycoprotein interaction with a putative cellular receptor, CD81. *J Virol* **73**:6235–
716 6244.
- 717 48. **Lindenbach BD, Evans MJ, Syder AJ, Wölk B, Tellinghuisen TL, Liu CC,**
718 **Maruyama T, Hynes RO, Burton DR, McKeating JA, Rice CM.** 2005. Complete
719 replication of hepatitis C virus in cell culture. *Science* **309**:623–626.

- 720 49. **Macdonald A, Crowder K, Street A, McCormick C, Saksela K, Harris M.** 2003.
721 The Hepatitis C Virus Non-structural NS5A Protein Inhibits Activating Protein-1
722 Function by Perturbing Ras-ERK Pathway Signaling. *J Biol Chem* **278**:17775–17784.
- 723 50. **Maillard P, Krawczynski K, Nitkiewicz J, Bronnert C, Sidorkiewicz M, Gounon**
724 **P, Dubuisson J, Faure G, Crainic R, Budkowska A.** 2001. Nonenveloped
725 nucleocapsids of hepatitis C virus in the serum of infected patients. *J Virol* **75**:8240–
726 8250.
- 727 51. **Catanese MT, Loureiro J, Jones CT, Dorner M, von Hahn T, Rice CM.** 2013.
728 Different Requirements for Scavenger Receptor Class B Type I in Hepatitis C Virus
729 Cell-Free versus Cell-to-Cell Transmission. *J Virol* **87**:8282–8293.
- 730 52. **Fofana I, Krieger SE, Grunert F, Glaubens S, Xiao F, Kremer SF, Soulier E,**
731 **Royer C, Thumann C, Mee CJ, McKeating JA, Dragic T, Pessaux P, Stoll-Keller**
732 **F, Schuster C, Thompson J, Baumert TF.** 2010. Monoclonal Anti-Claudin 1
733 Antibodies Prevent Hepatitis C Virus Infection of Primary Human Hepatocytes.
734 *Gastroenterology* **139**:953–964.e4.
- 735 53. **Biasini M, Bienert S, Waterhouse A, Arnold K, Studer G, Schmidt T, Kiefer F,**
736 **Gallo Cassarino T, Bertoni M, Bordoli L, Schwede T.** 2014. SWISS-MODEL:
737 modelling protein tertiary and quaternary structure using evolutionary information.
738 *Nucleic Acids Res* **42**:W252–8.
- 739 54. **Wakita T, Pietschmann T, Kato T, Date T, Miyamoto M, Zhao Z, Murthy K,**
740 **Habermann A, Kräusslich H-G, Mizokami M, Bartenschlager R, Liang TJ.** 2005.
741 Production of infectious hepatitis C virus in tissue culture from a cloned viral genome.
742 *Nat Med* **11**:791–796.

- 743 55. **Delgrange D, Pillez A, Castelain S, Cocquerel L, Rouille Y, Dubuisson J, Wakita**
744 **T, Duverlie G, Wychowski C.** 2007. Robust production of infectious viral particles in
745 Huh-7 cells by introducing mutations in hepatitis C virus structural proteins. *J Gen*
746 *Virol* **88**:2495–2503.
- 747 56. **Calland N, Albecka A, Belouzard S, Wychowski C, Duverlie G, Descamps V,**
748 **Hober D, Dubuisson J, Rouillé Y, Séron K.** 2012. (-)-Epigallocatechin-3-gallate is a
749 new inhibitor of hepatitis C virus entry. *Hepatology* **55**:720–729.
- 750 57. **Mederacke I, Wedemeyer H, Ciesek S, Steinmann E, Raupach R, Wursthorn K,**
751 **Manns MP, Tillmann HL.** 2009. Performance and clinical utility of a novel fully
752 automated quantitative HCV-core antigen assay. *J Clin Virol* **46**:210–215.
- 753 58. **Morota K, Fujinami R, Kinukawa H, Machida T, Ohno K, Saegusa H, Takeda K.**
754 2009. A new sensitive and automated chemiluminescent microparticle immunoassay
755 for quantitative determination of hepatitis C virus core antigen. *J Virol Methods*
756 **157**:8–14.
- 757 59. **Lavie M, Sarrazin S, Montserret R, Descamps V, Baumert TF, Duverlie G, Séron**
758 **K, Penin F, Dubuisson J.** 2014. Identification of conserved residues in hepatitis C
759 virus envelope glycoprotein E2 that modulate virus dependence on CD81 and SRB1
760 entry factors. *J Virol* **88**:10584–10597.
- 761 60. **Poenisch M, Metz P, Blankenburg H, Ruggieri A, Lee JY, Rupp D, Rebhan I,**
762 **Diederich K, Kaderali L, Domingues FS, Albrecht M, Lohmann V, Erfle H,**
763 **Bartenschlager R.** 2015. Identification of HNRNPK as Regulator of Hepatitis C Virus
764 Particle Production. *PLoS Pathog* **11**:e1004573.

765

766 **Figure legends**

767

768 **Figure 1: E1 N-terminal region sequence analyses.** The E1 aa 192–270 sequence from
769 HCV JFH1 strain (AB047639 ; genotype 2a) is indicated with respect to the polyproteins
770 numbering. (A) Secondary structure of E1 N-terminal 79 aa region. E1 sequence of JFH1
771 isolate with A4 epitope (specific of genotype 1a) engineered at its N-terminus (aa 197-207) is
772 presented. The secondary structures corresponding to the α -helix and β -strands previously
773 identified are highlighted in blue and yellow, respectively. Amino acid mutated in this study
774 are indicated by a red dot. (B) Amino acid repertoires of the N-terminal region of E1
775 ectodomain. The aa repertoire was deduced from the ClustalW multiple alignment of 19
776 reference sequences from all confirmed genotypes and subtypes (<http://www.euhcvdb.fr>).
777 Amino acids observed at a given position in fewer than two distinct sequences were not
778 included. Amino acids observed at a given position in more than 17 distinct sequences are
779 shown in capital letter. The degree of aa conservation at each position can be inferred from
780 the extent of variability (with the observed aa listed in decreasing order of frequency from top
781 to bottom) together with the similarity index according to ClustalW convention (asterisk,
782 invariant; colon, highly similar; dot, similar).

783

784 **Figure 2: Effects of mutations on viral protein expression and infectivity.** (A) Effects of
785 mutations on viral protein expression. Huh-7 cells were electroporated with viral RNA
786 transcribed from JFH1-derived mutants, and they were lysed at 48 h post-electroporation.
787 Viral proteins were separated by SDS-PAGE and detected by western blotting with MAbs A4
788 (anti-E1), 3/11 (anti-E2) and anti-NS5A. A western blotting analyzed with an anti-beta-
789 tubulin antibody was performed in parallel to verify that equal amounts of cell lysates had
790 been loaded. (B) Infectivity of E1 mutants. Huh-7 cells were electroporated with viral RNA

791 transcribed from JFH1-derived mutants. At 48, 72, and 96 h post-electroporation, infectivities
792 of the supernatants and intracellular viruses were determined by titration. Error bars indicate
793 standard errors of the mean (SEM) from at least three independent experiments. $P < 0.05$ for
794 intracellular mutants Q193A, V194A, I212A, T213A, W214A, Q215A, V220A, L221A,
795 H222A, R231A, G233A, W239A, V240A, P244A, I262A, D263A and M264A. $P < 0.05$ for
796 extracellular mutants I212A, T213A, W214A, Q215A, H222A, W239A and D263A.

797

798 **Figure 3: Analysis of core protein release for E1 mutants.** Huh-7 cells were electroporated
799 with viral RNA transcribed from JFH1-derived mutants. At 48 h postelectroporation, the
800 amount of intracellular core antigen was determined in cell lysates (A), as well as in
801 supernatants (B). A control experiment with a genome defective in virus assembly, Δ E1E2, is
802 shown in panel C. HCV core was quantified by a fully automated chemiluminescent
803 microparticle immunoassay. Error bars indicate SD. $P < 0.05$ for extracellular mutants I212A,
804 T213A, W214A, Q215A, H222A and W239A.

805

806 **Figure 4: Effect of E1 mutations on HCV glycoproteins folding and E1E2**
807 **heterodimerization.** (A) Interaction of viral glycoproteins with HCV entry factor CD81. At
808 48h post-electroporation, lysates were analyzed by GST pulldown using CD81-LEL-GST
809 fusion protein. Pulled-down E1 and E2 were analyzed by SDS-PAGE and detected by
810 western blotting with MAbs A4 and 3/11. (B and C) Interaction of HCV glycoproteins with
811 the conformation-sensitive anti-E1E2 Mab AR5A (B) and anti-E1 Mab IGH526 (C). At 48h
812 post-electroporation, E1 and E2 from cell lysates were analyzed by immunoprecipitation with
813 Mabs AR5A and IGH526. Precipitated E1 and E2 were then separated by SDS-PAGE and
814 detected by western blotting with Mabs A4 and 3/11. The weaker E1 signal observed with

815 two of our mutants (Q193A and V194A) is likely due to the involvement of these two
816 residues in A4 epitope.

817

818 **Figure 5: Effect of E1 mutations on sensitivity to antibody neutralization and inhibition**

819 **by CD81.** CD81 inhibition assays (A), AR5A neutralization experiments (B) and IGH526

820 neutralization experiments (C), were performed by incubating E1 mutants or WT virus with

821 increasing concentrations of human CD81-LEL, Mab AR5A or Mab IGH526. After 2 h of

822 incubation at 37°C, the mixtures were put into contact with target cells, and the inoculum was

823 replaced by fresh medium at 6h post-infection. At 72h post-infection, residual infectivity was

824 measured by immunofluorescence. The values are the combined data from three independent

825 experiments. The error bars represent SEM. $P < 0.05$ for mutants T213A and I262A in all

826 inhibitory conditions.

827

828 **Figure 6: Effect of E1 mutations on the recognition of HCV receptors.** Huh-7 cells were

829 pre-incubated for 2h at 37°C with increasing concentrations of antibodies targeting HCV

830 receptors: anti-CD81 Mab JS81 (A), anti-SR-BI Mab C167 (B), anti-CLDN1 Mab OM8A9-

831 A3 (C) or anti-CLDN6 Mab 342927 (D). Cells were then incubated with E1 mutants or WT

832 virus, and the inoculum was replaced by fresh medium at 6h post-infection. At 72h post-

833 infection, cells were processed for immunofluorescence to quantify the residual infectivity.

834 The values are the combined data from three independent experiments. The error bars

835 represent SEM. $P < 0.05$ for mutants T213A and I262A in the presence of anti-CLDN1 and

836 anti-CLDN6 antibodies. (E) Effect of E1 mutations on the recognition of CLDN1 and

837 CLDN6. Huh-7 cells were pre-incubated for 2h at 37°C with a combination of anti-CLDN1

838 (5 µg/ml) and anti-CLDN6 (10 µg/ml) Mabs. Cells were then incubated with E1 mutants or

839 WT virus, and the inoculum was replaced by fresh medium at 6h post-infection. At 72h post-

840 infection, cells were processed for immunofluorescence to quantify the residual infectivity.
841 The values are the combined data from three independent experiments. The error bars
842 represent SEM.

843

844 **Figure 7: Characterization of the secreted form of D263A mutant.** Concentrated
845 supernatant of cells electroporated with HCV were separated by sedimentation through a 10-
846 50% iodixanol gradient. Fractions were collected from the top and analyzed for their
847 infectivity as well as their viral RNA (A) and core protein content (B). (C) Analyses of
848 intracellular genomic replication for D263A mutant. Intracellular HCV genome copies in
849 electroporated cells were quantified at different times post-electroporation. Control
850 experiments with WT and Δ E1E2 and GND mutants were performed. The error bars
851 represent SD.

852

853 **Figure 8: Analysis of core protein oligomerization by velocity sedimentation.** Cells
854 electroporated with D263A mutant, Δ E1E2 or wild-type JFH1 RNA genomes were lysed at
855 48 h post-electroporation. Lysates were subjected to velocity sedimentation on a 10 to 50%
856 iodixanol density gradient, followed by western blot analysis of core protein. Fractions were
857 collected from the top. A control gradient was performed in parallel with extracts of cells
858 electroporated with the wild-type genome that had been treated with 1% SDS (lower panel).
859 The input represents 8% of lysates.

860

861 **Figure 9: Subcellular localization of HCV proteins in the context of D263A mutant.**
862 Electroporated cells grown on coverslips were fixed at 48h post-electroporation and
863 processed for immunofluorescence with antibodies against viral proteins (E1, E2, core or
864 NS5A). Lipid droplets were stained with BODIPY 493/503 (green). Rat anti-E2 Mab 3/11

865 was used for the colocalization with E1 (mouse anti-E1 Mab A4). Anti-core Mab ACAP27
866 was used for the colocalization with lipid droplets (LD). The NS5A protein was labeled with
867 anti-NS5A (9E10). Nuclei were stained with DAPI (blue). Representative confocal images of
868 individual cells are shown with the merge images in the right column. Bar, 25 μ m.

869

870 **Figure 10: Subcellular localization of D263A mutant and wild-type RNA by fluorescent**
871 ***in situ* hybridization (FISH).** Huh-7 cells were electroporated with D263A and wild-type
872 (WT) RNA genomes, fixed at 48h post-electroporation and processed for HCV positive
873 strand specific RNA detection, followed by immunofluorescence staining for core with Mab
874 ACAP27 (A) or for E1 with Mab A4 (B). Scale bar is 20 μ m. (C) Pearson's correlation
875 coefficient. Error bars represent standard deviation from 21 different images (***) p =
876 0.0004).

877

878 **Figure 11: Position of identified amino acid residues on the 3D structure of E1 N-**
879 **terminal region.** The residues identified in this study are highlighted on the structural model
880 of the N-terminal region of E1 from the JFH1 isolate. This model was built using the Swiss-
881 Model web server (53) with the crystallographic structure of E1 (H77 strain) (PDB code
882 4UOI) as template. (A) Residues for which the mutation toward an alanine showed an
883 interesting or lethal phenotype are colored in green and orange respectively and their side
884 chain shown as stick. (B) Hydrogen bonds network established by the D263 residue with
885 others residues from the β 4 and β 5 strands. The figure was generated using the PyMOL
886 Molecular Graphics System, Version 1.8 Schrödinger, LLC.

887

A

192 200 210 220 230 240 250 260 270

| | | | | | | | |

E1_JFH1 **AQVKNTSSSYMVTNDCS****ND**SITWQ**LEAAVLHV**PGCV**P**C**ER**-V**GNT****SRCWVPV**SPNMAVRQPGALTQGLRT**HIDMVV**MSAT

β1 β2 α β3 β4 β5

* * * ****.. *: : ::* .***: .. ** : ::: .* :: :. ..

vevrNsSgiYhlTNDcSNsSIvyeaedailHlPGCVPCvr-egNtSrCWvpvtPtlAvrnagaptaglRrHvDllvgaAt
 lqya a sl mv p a twqldaivm t ek tn a s tals nv apysvlarsf t i miams a
 yh k t v a n l taam v i d q t hqaa i ikqr tis i s m a v
 n g i s gv v g isi t ds vt v
 t k l i l h k

B

Amino acid repertoire




Fig 1

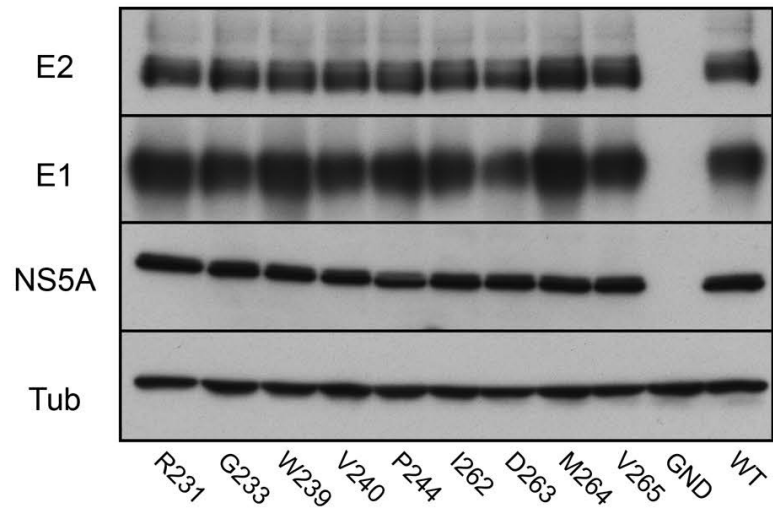
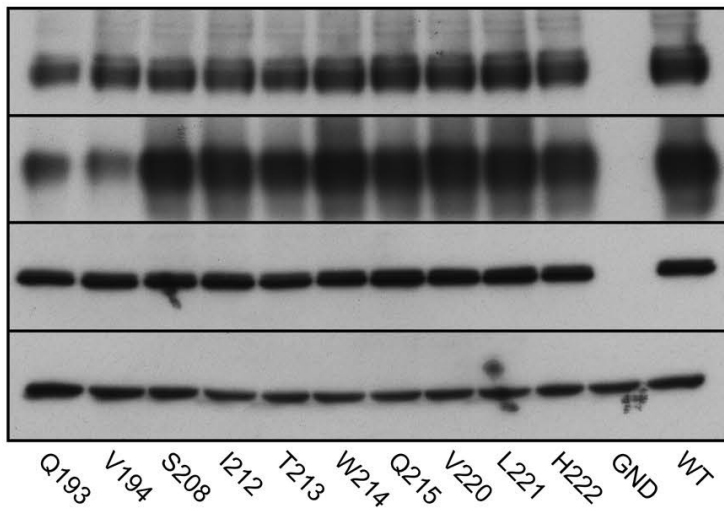
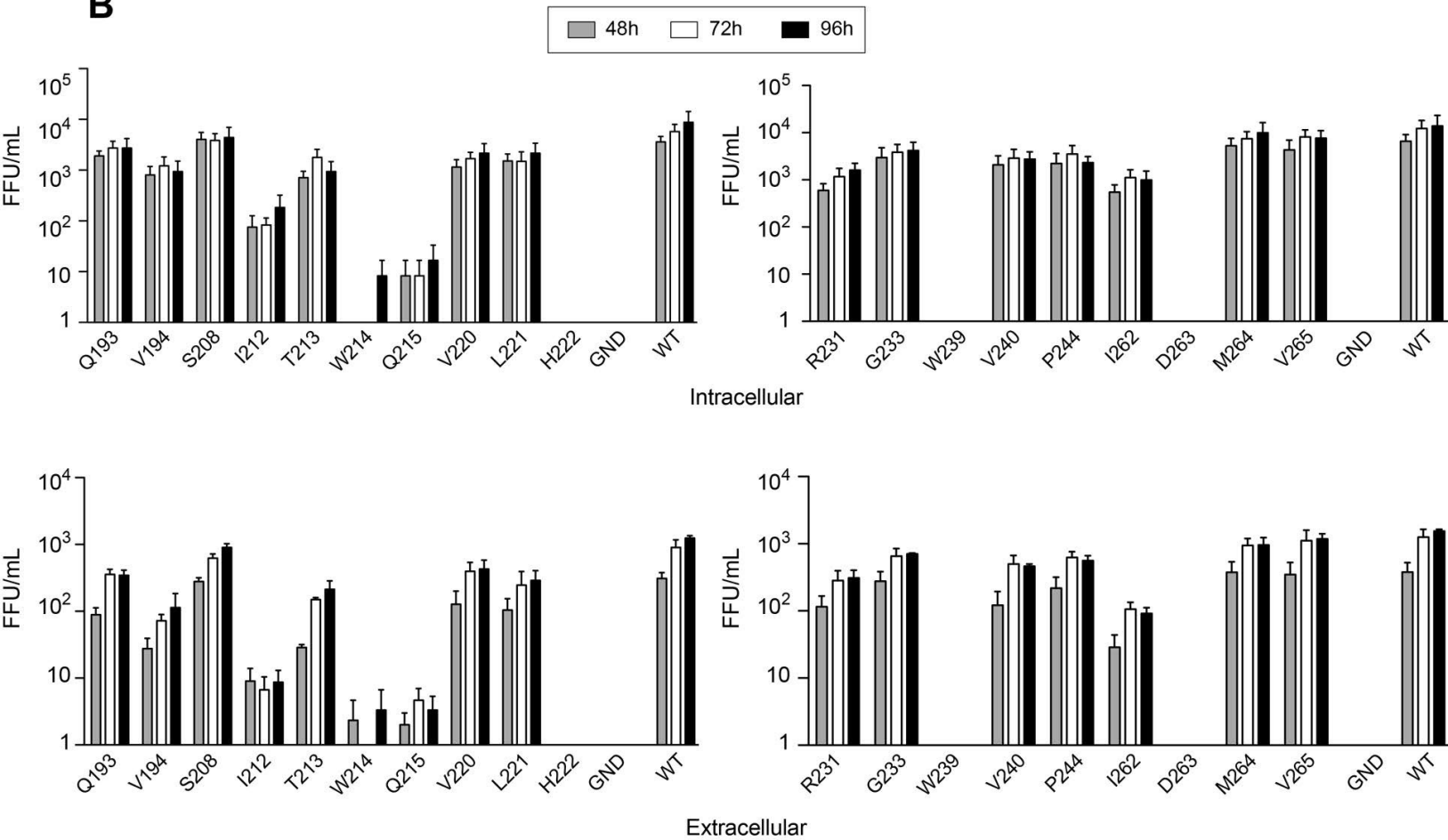
A**B**

Fig 2

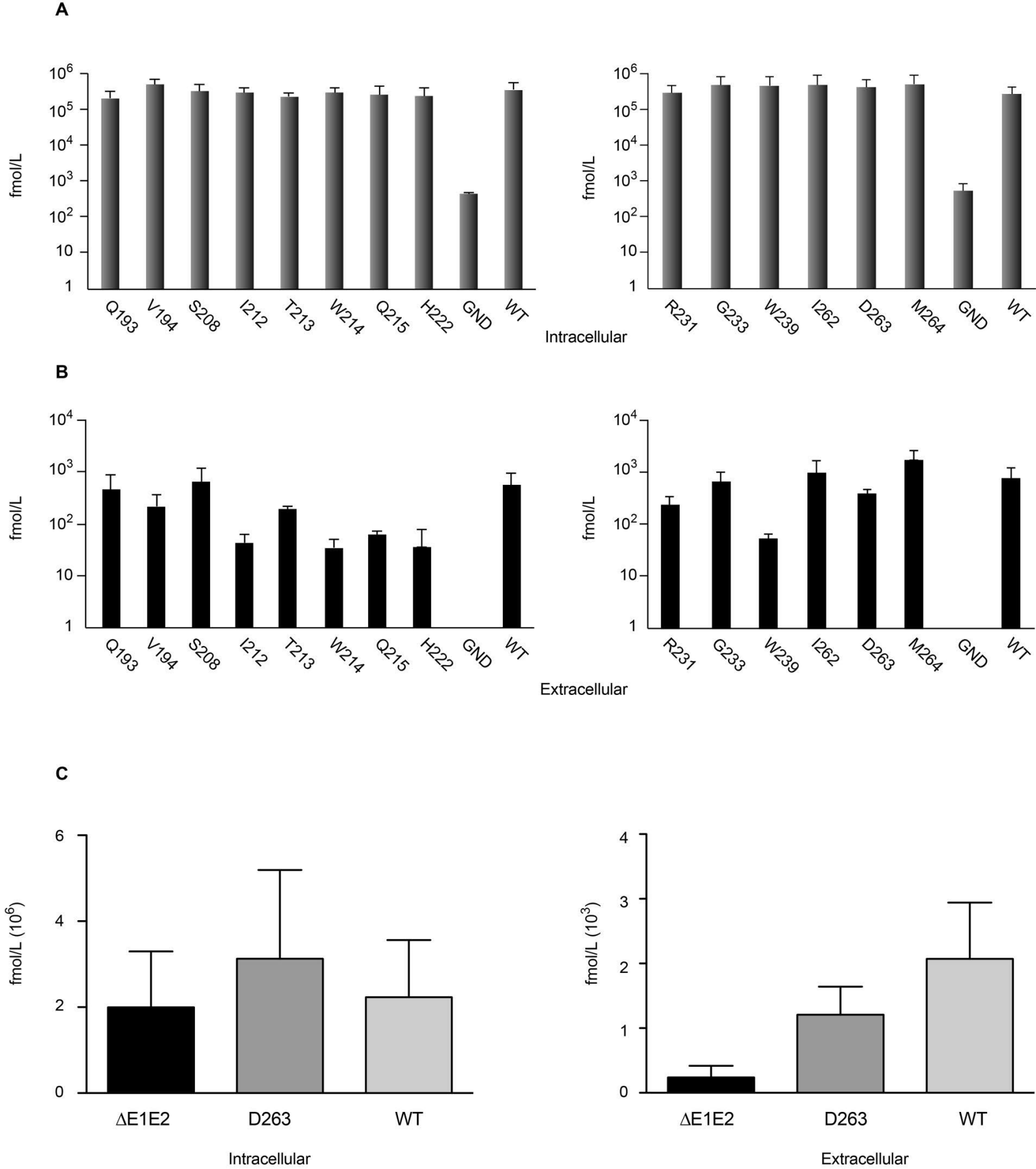


Fig 3

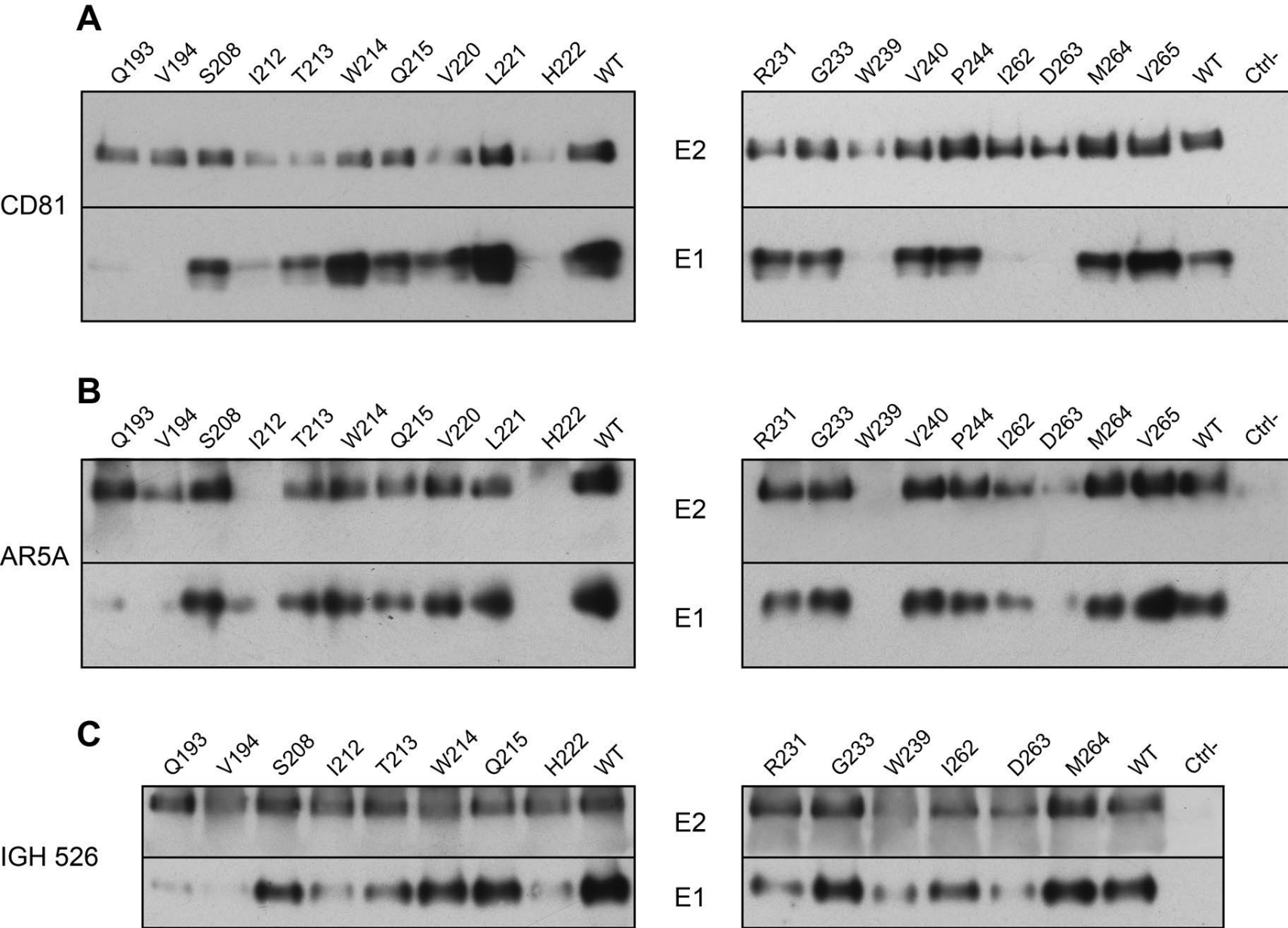


Fig 4

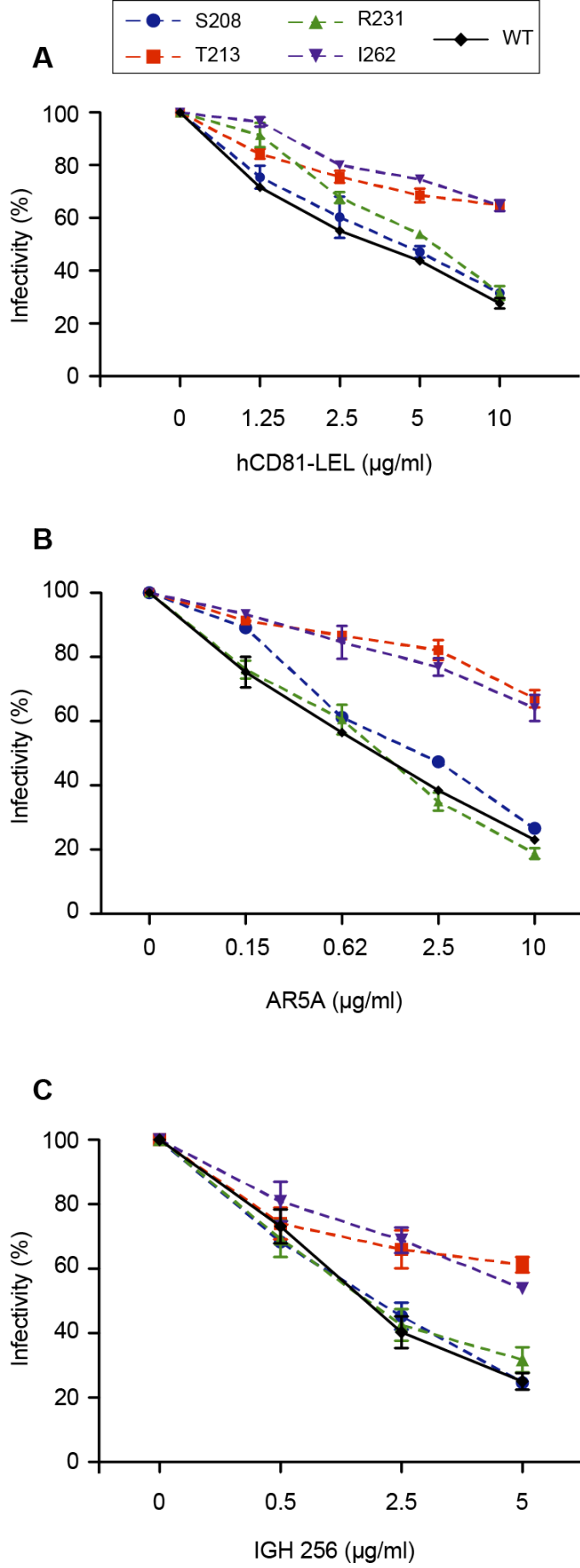


Fig 5

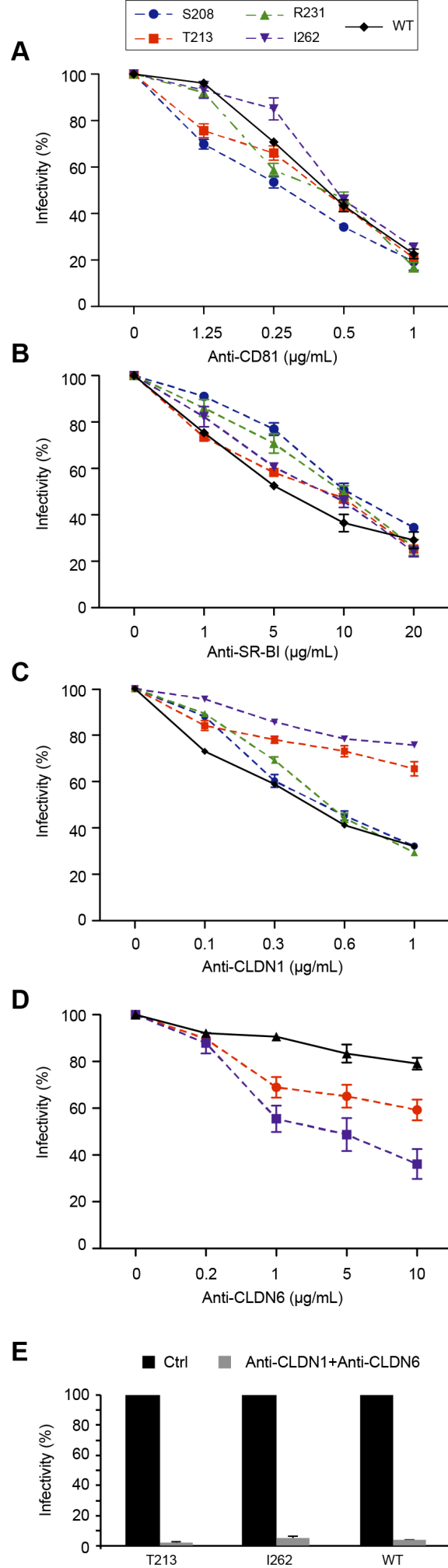


Fig 6

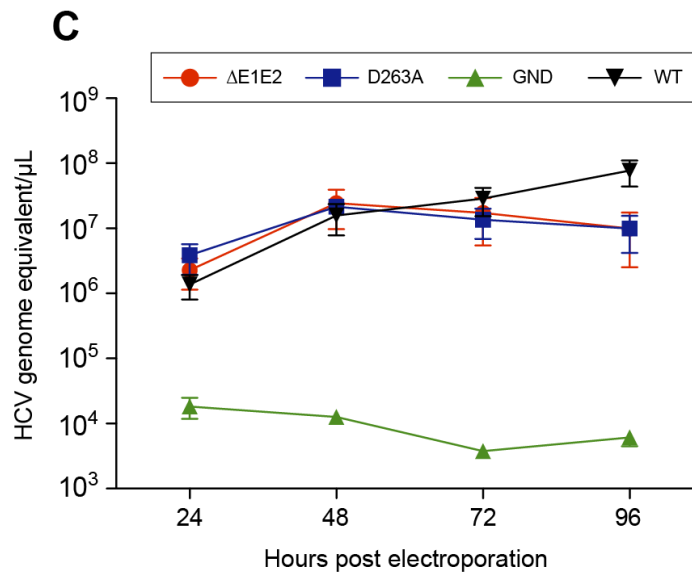
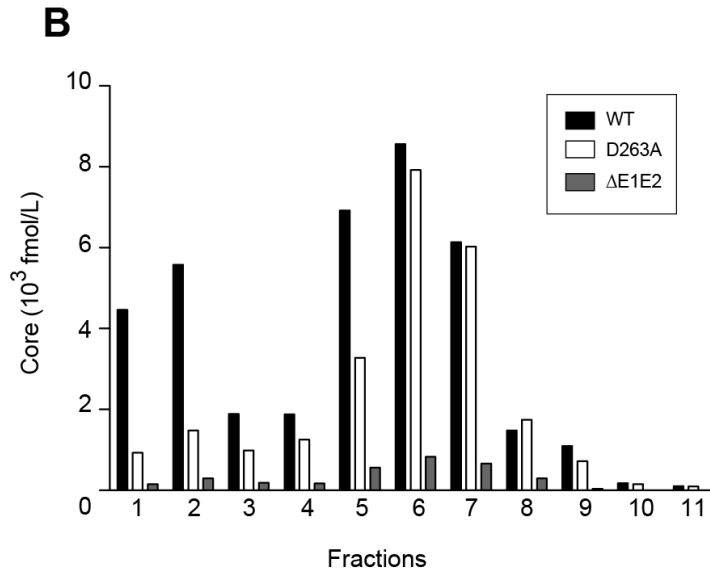
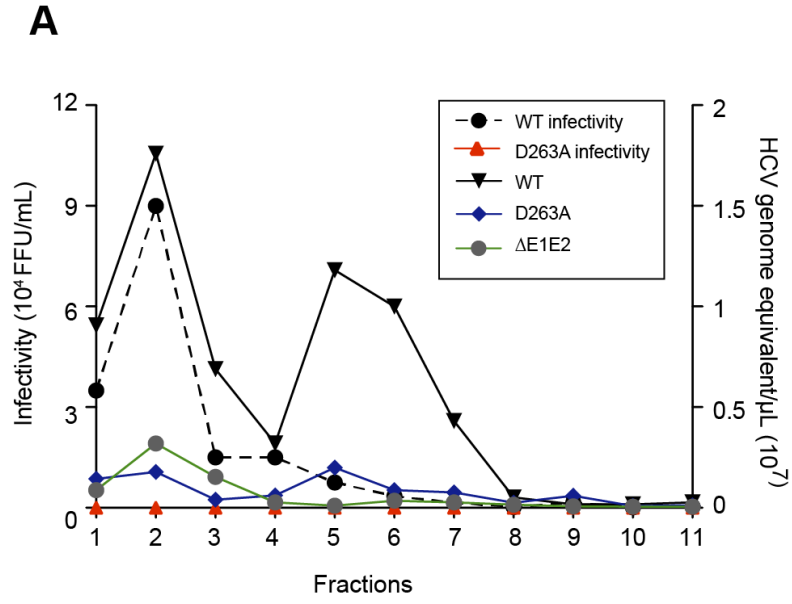


Fig 7

Fractions (from top to bottom)

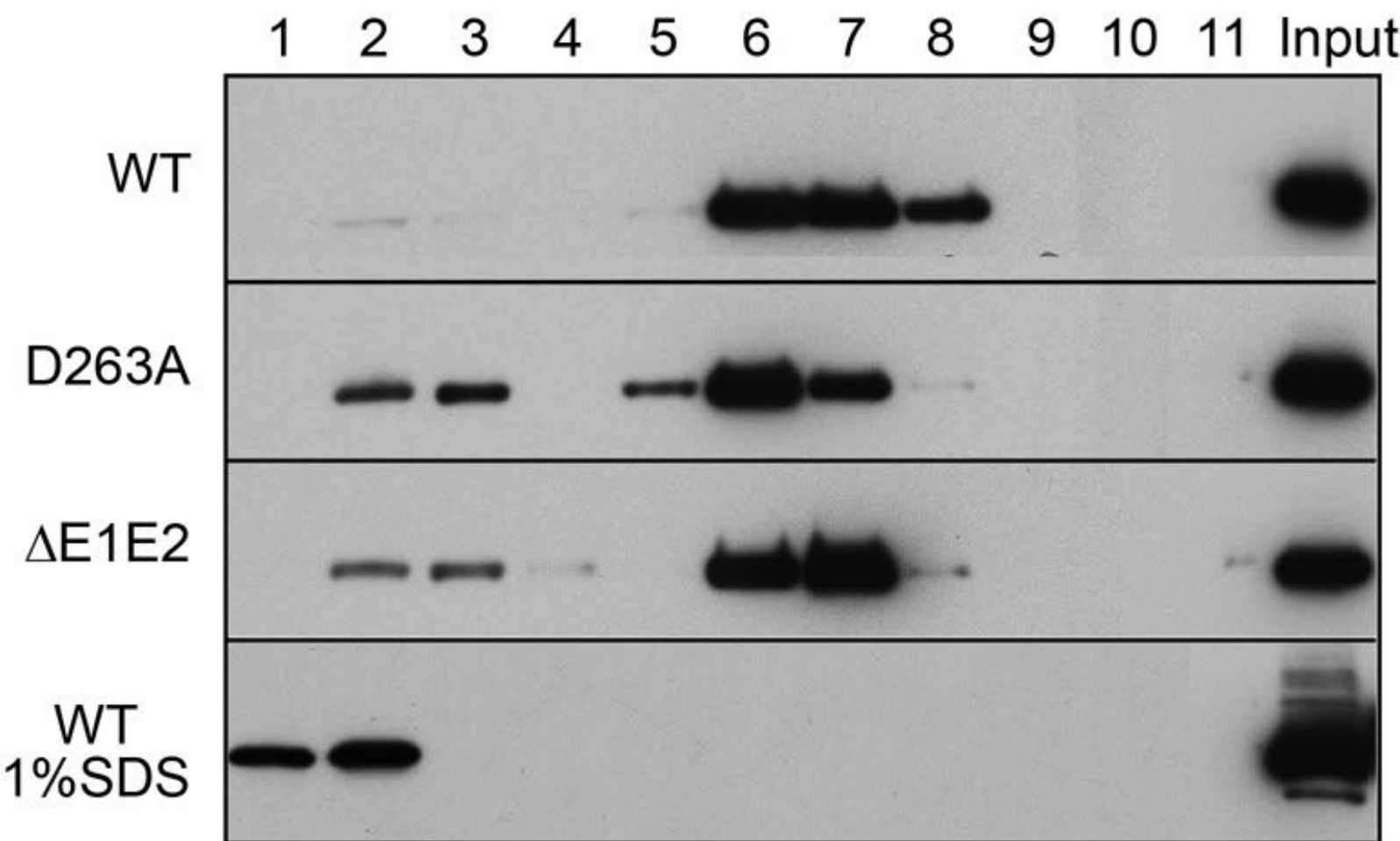


Fig 8

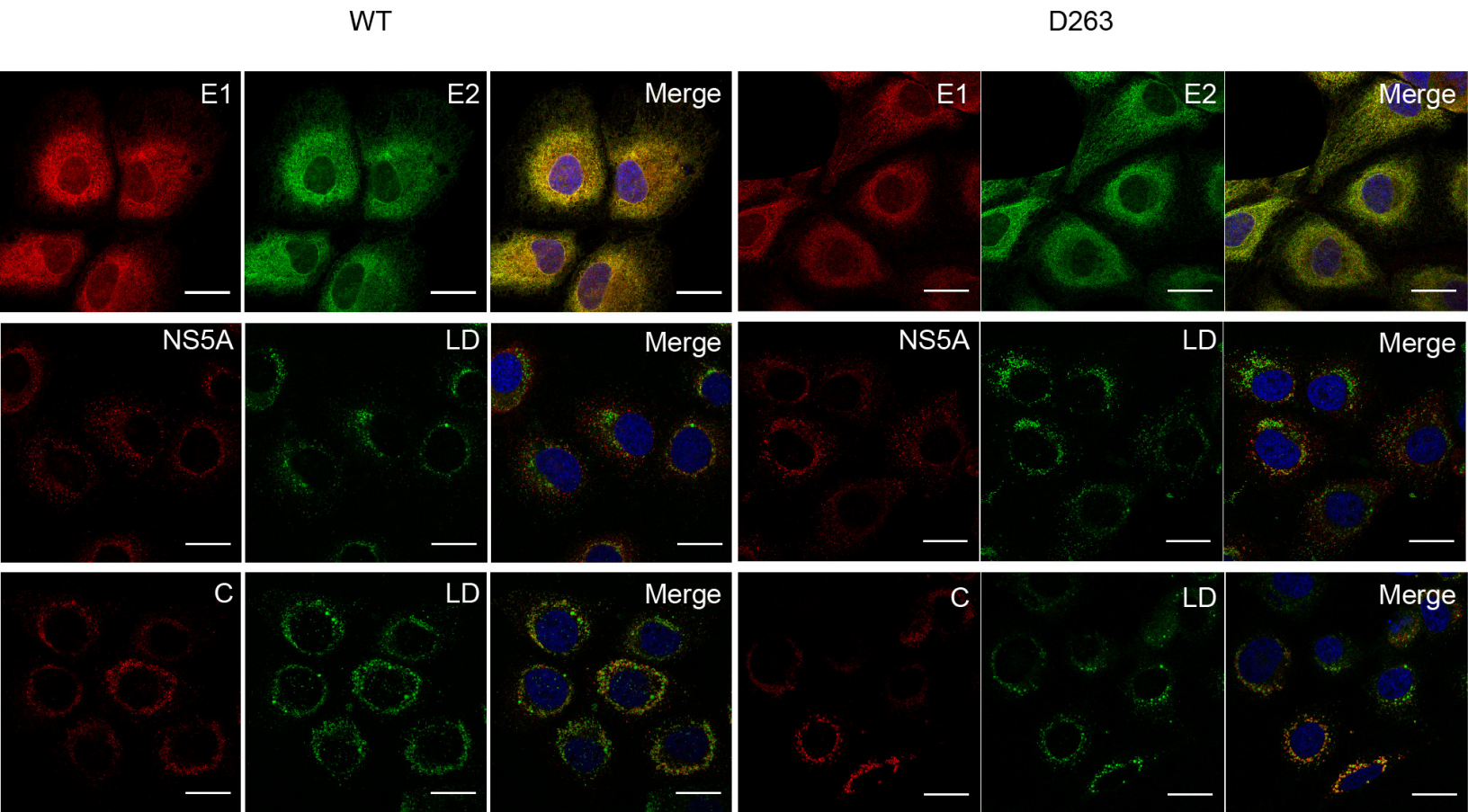


Fig 9

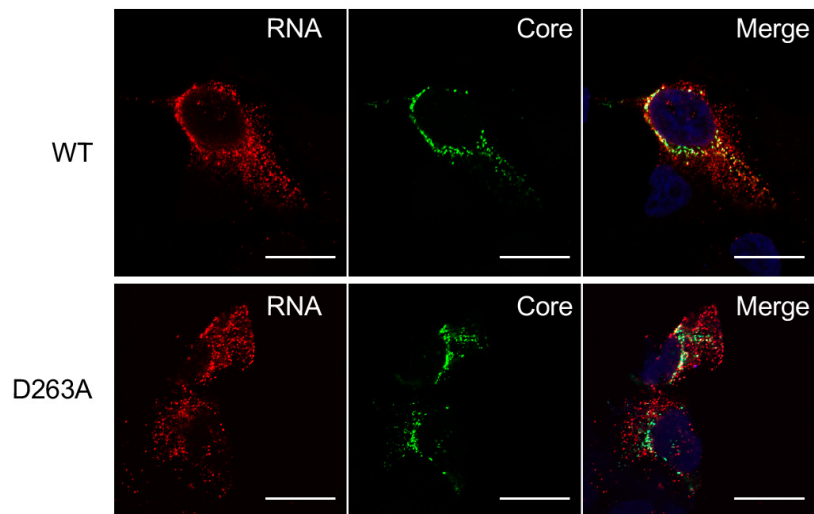
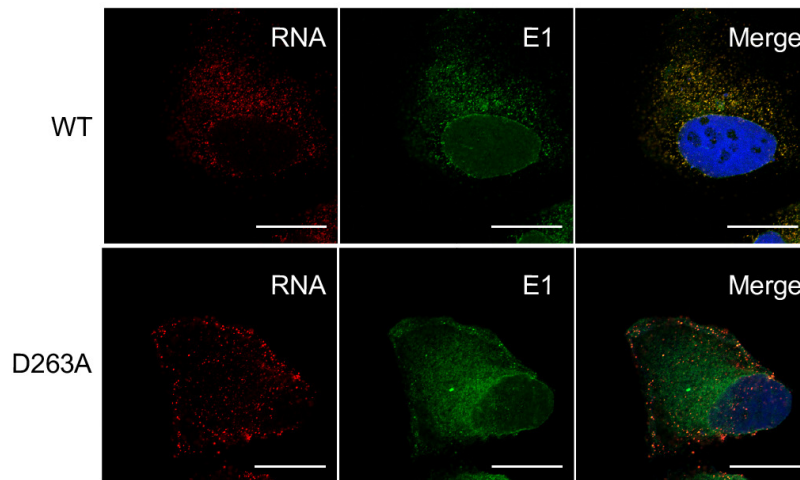
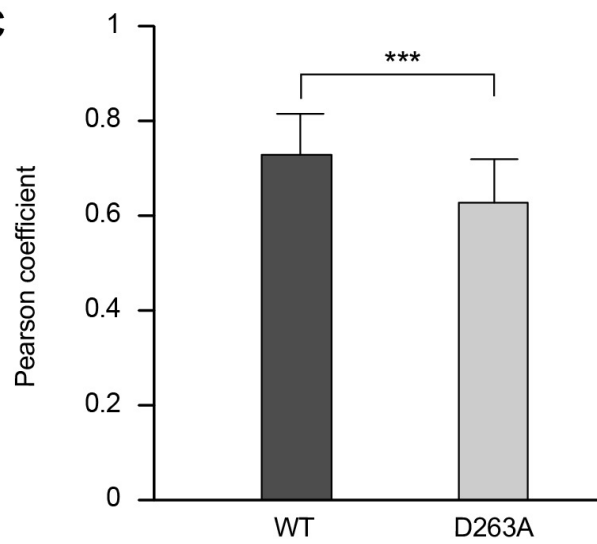
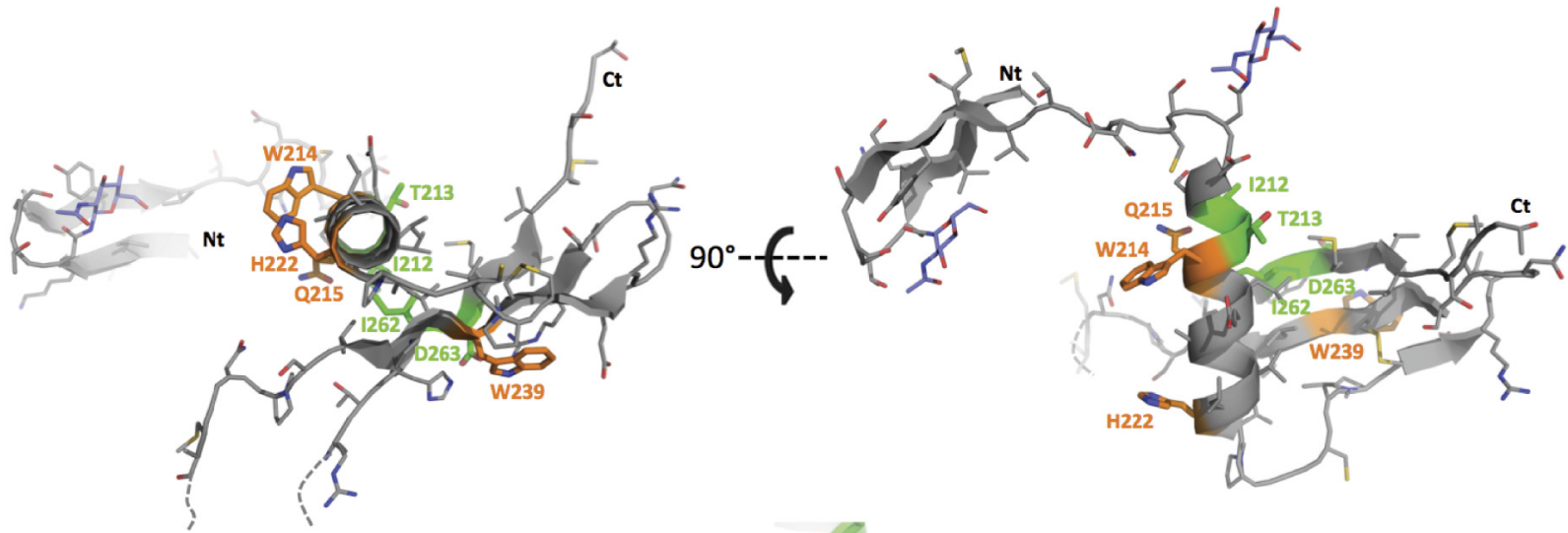
A**B****C**

Fig 10

A



B

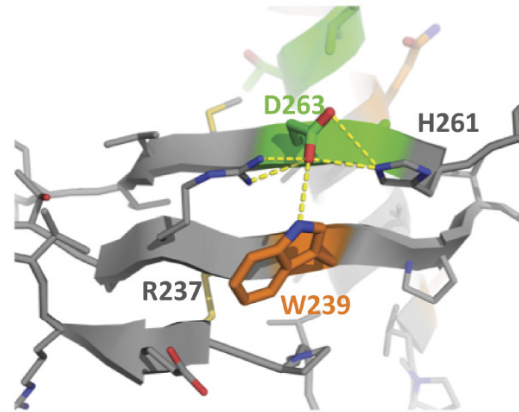


Fig 11